NTNU

Norwegian University of
Science and Technology

Analysis of the Metabolic Response of *Saccharomyces Cerevisiae* to DNA Damaging Agents

Simon Scheel Rey

Chemical Engineering and Biotechnology
Submission date: June 2011
Supervisor: Per Bruheim, IBT

Norwegian University of Science and Technology
Department of Biotechnology

Declaration

I hereby declare that this Master thesis in Biotechnology is completed in accordance with all the rules and regulations of the Norwegian University of Science and Technology.

_____

Simon Scheel Rey

Trondheim, June 20 - 2011

Acknowledgments

The experiments for this work were performed in the laboratories of NTNU, the Department of Biotechnology.

I would like to thank my supervisor Associate Professor Per Bruheim for his inspiring guidance, and for always showing an interest in my work.

I would also like to thank Anne Marte Haug for a great partnership in the laboratory, Kåre A. Kristiansen, PhD, for teaching me how to operate the fermenter and helping me with the GC – MS, and anyone else that has answered any questions during my work in the laboratory.

A special thanks to Fredrik and Lene Kristin for our special friendship and for your support.

Finally, I would like to thank my family for all their love and support that has kept me going all these years.

Abstract

Saccharomyces cerevisiae, commonly known as Baker's yeast, is a eukaryotic model organism widely used in biotechnology research. Its genome has a high degree of similarity to humans, and research done on *S. cerevisiae* can give us a better understanding of the mechanisms involved and the cellular responses to anti-cancer drugs.

The main goal for this master thesis was to investigate the metabolic response of *S. cerevisiae* to DNA damaging agents. Methods for cultivation of *S. cerevisiae* in shake flasks or in a bioreactor, for sampling and extraction of cells, and for analysis of the sample using GC – MS were developed. A custom Deconvolution Reporting Software library was created, and used to analyze the metabolic response of *S. cerevisiae* to 5-fluoruracil (5FU), a widely used anti-cancer drugs. The publicly available software FiatFlux 1.6X was used for metabolic flux analysis of *S. cerevisiae* grown in medium containing labeled [U-^{13}C]-glucose and in the presence of 5-fluorouracil or methyl methanesulfonate (MMS), a model alkylating agent.

An overall decrease in the amount of intracellular metabolites was observed as a response to addition of a growth-inhibiting dose of 5FU, while no clear response was observed for a lower, more tolerable dose. Growth of *S. cerevisiae* under the presence of 5FU resulted in a different cellular response than growth under the presence of MMS. The presence of both DNA-damaging agents resulted in a decrease in the ratio of the fluxes leading to mitochondrial acetyl-CoA compared to an unstressed culture, possibly indicating a reduction in the activity of the TCA cycle. The 5FU stressed cells showed an increase in conversion of fumarate to oxaloacetate and the subsequent export out of the mitochondrion, while the MMS stressed cells showed a decrease of this flux.

The experimental methods can be further refined to obtain data of higher quality, and thus allow a more complete metabolic profile to be created. The conditions for derivatization can be optimized to ensure a complete derivatization of all metabolites, the DRS library can be expanded to include a wider range of metabolites, and experiments of stressing the cells performed in a chemostat can eliminate any effects the differences in specific growth rates might have on the metabolome or fluxome of *S.cerevisiae*.

Contents

1 Introduction

1.1 Saccharomyces cerevisiae

Saccharomyces cerevisiae is a eukaryotic microorganism and part of the fungi kingdom, belonging to the order *Saccharomycetales.* It has been used in the production of food and beverages for hundreds of years, particularly in brewing of beer and in baking (hence the more common name: Baker's yeast). It was the first eukaryote to have its full genome sequenced (Goffeau, Barrell et al. 1996), and comparison of the genes in *S. cerevisiae* and humans revealed that 36.6 % of the genes in the yeast are homologues (they share a common ancestor) to genes in humans (Berglund, Sjölund et al. 2008). *S. cerevisiae* is easily cultivated under controlled conditions, which is vital for the reproducibility of studies, and its DNA is easily manipulated. It is non-pathogenic and classified as a GRAS (generally regarded as safe) organism, and the extensive research done on this organism has earned it a role as a eukaryotic model organism. Genes from humans or other eukaryotes can be expressed in *S. cerevisiae* (Melese and Hieter 2002), allowing studies that normally would not be possible due to ethical dilemmas or technical difficulties. It has been genetically modified to produce a wide variety of substances of commercial interest. Human interferon was the first recombinant protein to be produced by *S. cerevisiae* in 1981 (Hitzeman, Hagie et al. 1981). Other examples include production of hydrocortisone by introduction of genes from higher eukaryotes into the yeast (Szczebara, Chandelier et al. 2003), introduction of fermentative pathways from other microorganism to enable the fermentation of xylose (Karhumaa, Garcia Sanchez et al. 2007), and the increased production of succinate by deletions of genes encoding specific enzymes in the tricarboxylic acid cycle (TCA) (Karhumaa, Garcia Sanchez et al. 2007).

S. cerevisiae is unicellular, has a round to ovoid shape with a diameter of approximately 5 µm. It can be either haploid (single set of unpaired chromosomes) or diploid (a pair of each type of chromosomes). The cells normally undergo mitosis; however, meiosis can occur during the diploid state, returning the cells to the haploid phase. Reproduction in yeast occurs by "budding", a form of reproduction in which a new cell, the daughter cell, emerges from the mother cell. Budding cells of *S. cerevisiae* are shown in Figure 1-1.

Figure 1-1: An electron micrograph of budding cells of *Saccharomyces cerevisiae* (Phyterra yeast Inc. 2011).

Before mitosis begins the DNA of the parent cell duplicates into two copies of the 16 chromosomes. These two identical copies are known as sister chromatids. As mitosis begins, the sister chromatids are separated. One will remain in the parent cell, while the other migrates into the newly formed bud. As the bud matures, it will eventually separate from the parent cell forming a new, independent cell. The complete cell cycle of yeast is shown in Figure 1-2.

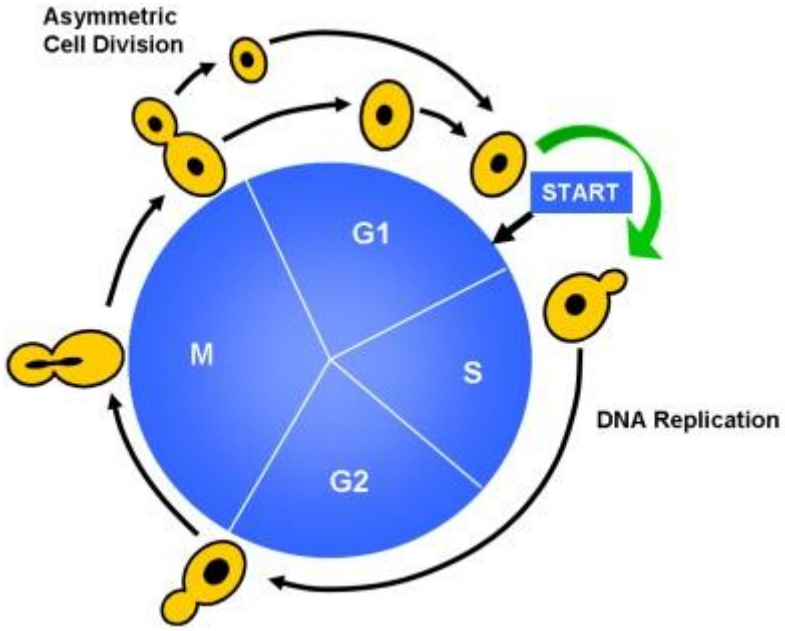

Figure 1-2: The cell cycle of *S. cerevisiae* and the key transition point for replication start. The cycle consists of the Synthesis phase, two Gap phases, and the Mitotic phase (Adapted from Swiss Federal Insitute of Technology Zürich 2008).

The cell cycle is regulated at a key transition point called **start**. The condition of the cell at this point determines whether a new round of replication should be initiated or not. This transition point is influenced by factors like available nutrients, the size of the cell, and DNA damage. As replication starts, the cell enters the synthesis phase (S), where new DNA is synthesized. Two gap phases (G1 and G2) separate the S-phase from the mitiotic phase (M).

The gametes of yeast can be of either of two mating types. The mating type of the haploid cell is determined by the genes at the *ma*ting-*t*ype locus, *MAT*. These genes can be either of **a**-type or α-type, and they are regulators of other genes involved in mating. A cell expressing the α-type proteins can only mate with cells expressing the **a**-type proteins, and vice versa, thus creating **a**/α-diploid cells. Haploid cells can switch between the two mating types as often as every generation. An overview of the life cycle of *S. cerevisiae* is shown in Figure 1-3.

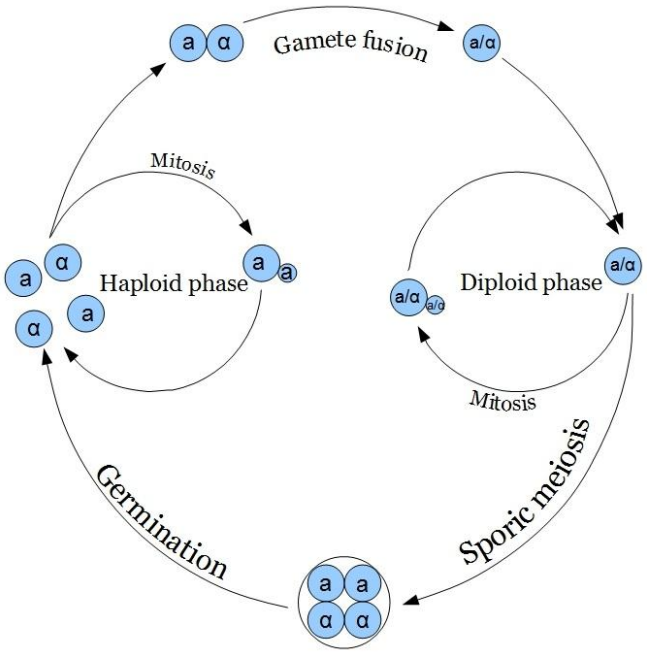

Figure 1-3: The life cycle of *S. cerevisiae*. The common form of reproduction is by mitosis, either as a haploid or a diploid. Reproduction by meiosis will convert the cells from a diploid state to a haploid state (Adapted from Lab Dom AVMM (Suisse) Inc. 2011).

As with all life forms, the genome of *S. cerevisiae* is under constant attack from both endogenous and exogenous sources. The maintenance of the DNA is vital to ensure cell viability and genomic stability, and eukaryotes can repair their DNA by different pathways. The major pathways are homologous recombination repair (HRR), non-homologous end-joining (NHEJ), base excision repair (BER), nucleotide excision repair (NER), mismatch repair (MMR), and methyltransferase repair (Lopez-Camarillo, Lopez-Casamichana et al. 2009). These pathways have been thought to be highly conserved within eukaryotes and even from bacteria to higher eukaryotes (Taylor and Lehmann 1998). All components in the NER and HRR pathways have sequence homologues conserved between yeast and humans, whereas this is not the case in BER. However, BER genes from one organism can complement genes of similar function in other organisms (Taylor and Lehmann 1998). Some crucial proteins in the NHEJ pathway in mammals have no sequence homologues in yeast, but an increasing number of proteins in yeast with almost identical three-dimensional structure to these mammalian proteins have been found (Taylor and Lehmann 1998). Although there are many similarities in the DNA repair pathways in humans and yeast, recent research has uncovered some important disparities. The BER pathway is essential for repairing DNA damage caused by alkylating agents, and significant differences from *S. cerevisiae* to humans in both structure and function of the proteins involved have been revealed (Kelley, Kow et al. 2003). Evidently, *S. cerevisiae* is useful for modeling higher eukaryotes like humans, but further research is required to fully understand the relationship between the two eukaryotes.

1.2 DNA damaging agents

Cancerous tumors can generally be differentiated from benign tumors by three main properties; uncontrolled growth, invasion and destruction of adjacent tissue, and spreading to other parts of the body by transport through the blood or the lymph. The division of cells occurs rapidly, and most anti-cancer drugs have been designed with this property in mind. The quickly dividing cancer cells have less time to react to the damage introduced by the anti-cancer drug than normal cells, and a larger proportion of the targeted cells are undergoing cell division at any time. Other quickly dividing cells in the human body are also sensitive to the anti-cancer drugs, such as the cells responsible for hair growth, which is the reason for the characteristic hair loss of patients undergoing chemotherapy.

The type of cancer to be treated determines which anti-cancer drug is used, depending on their mechanism of action. The most common are *alkylating agents* that chemically modify the cells' DNA, *anti-metabolites* that prevent the synthesis of DNA during the synthesis phase of

the cell cycle, *plant alkaloids* that prevent microtubule function, and *topoisomerase inhibitors* that inhibit the enzymes responsible for DNA topology. To improve the effectiveness of anti-cancer drugs, research is being done on model organisms like *S. cerevisiae* to give a better understanding of the mechanisms involved and the cellular responses to these drugs.

1.2.1 5-fluorouracil

5-fluorouracil (5FU) is an anti-metabolite drug that has been in use since the 1950s in treatment of colorectal and breast cancers, and cancers of the aerodigestive tract (Longley, Harkin et al. 2003). It inhibits cell growth by two mechanisms, inhibition of important biosynthetic processes and incorporation into DNA and RNA.

5FU is an analogue of uracil. At the C-5 position of uracil a hydrogen atom is replaced with a fluorine atom (Figure 1-4).

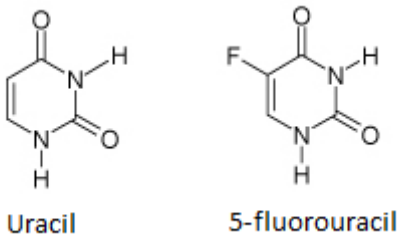

Figure 1-4: The molecular structure of uracil and its analogue 5-fluorouracil.

It enters the cell by the same facilitated transport systems as uracil (Wohlhueter, McIvor et al. 1980). Inside the cell 5FU is converted to different metabolites similarly to uracil, and these metabolites are directly involved in the mechanisms that disrupt cell growth (Longley, Harkin et al. 2003). An overview of the mechanisms of action of 5FU is shown in Figure 1-5.

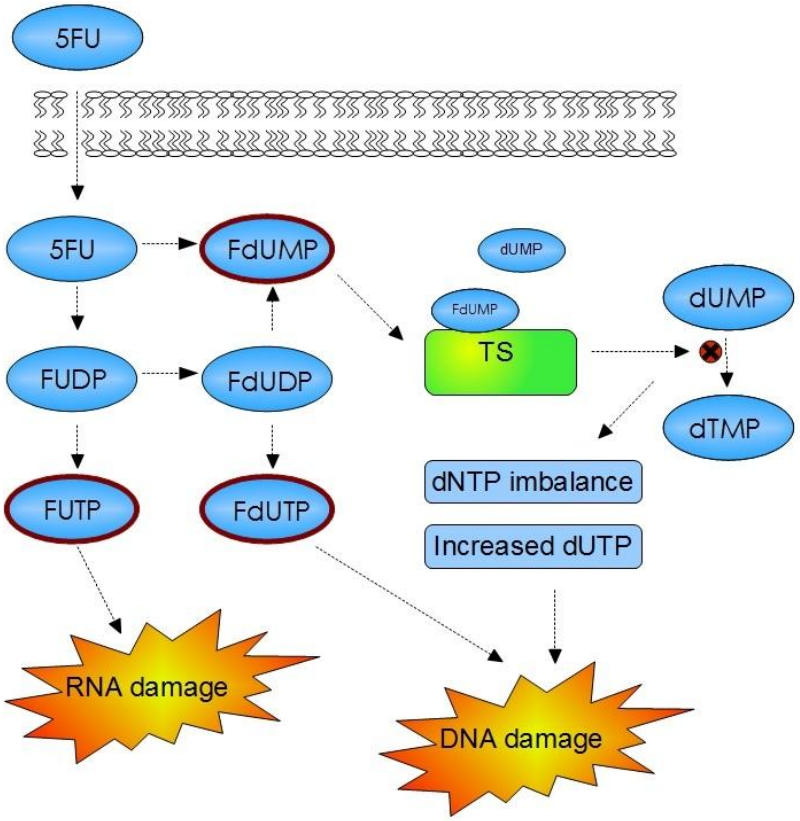

Figure 1-5: Metabolism of 5FU and the mechanisms of the anti-cancer effects of its metabolites. The three active metabolites (highlighted by a dark red border) are fluorourdine triphosphate (FUTP), fluorodeoxyuridine monophosphate (FdUMP) and fluorodeoxyuridine triphosphate (FdUTP) (Adapted from Longley, Harkin et al. 2003).

Fluorouridine phosphate (FUTP) is converted from 5FU via fluorouridine monophosphate (FUMP, not shown) and fluorouridine diphosphate (FUDP). FUDP can be converted to fluorodeoxyuridine diphosphate (FdUDP), which in turn can either be phosphorylated to fluorodeoxyuridine triphosphate (FdUTP) or dephosphorylated to fluorodeoxyuridine monophosphate (FdUMP). FdUMP can alternatively be converted from 5FU via phosphorylation of fluorodeoxyuridine (FUDR, not shown).

Misincorporation of FUTP into RNA will lead to inhibition of formation of mature rRNA from pre- rRNA (Ghoshal and Jacob 1994), disruption of post-transcriptional modification of

tRNA (Santi and Hardy 1987), and inhibition of splicing of pre-mRNA (Patton 1993). All these effects are toxic to the cell and lead to lowered cellular metabolism and viability.

FdUMP is an inhibitor to thymidylate synthase (TS), the enzyme responsible for the sole *de novo* source of deoxythymidine monophosphate (dTMP). TS catalyzes the methylation of deoxyuridine monophosphate (dUMP) forming dTMP, but binding of FdUMP to the nucleotide-binding site of TS blocks the binding of dUMP, the normal substrate, thus reducing the production of dTMP. The consequence of this inhibition is depletion of dTMP, and subsequently, depletion of deoxythymidine triphosphate (dTTP). This causes an imbalance in the deoxynucleotide pool which can disrupt DNA synthesis and repair, with fatal consequences to the cell (Yoshioka, Tanaka et al. 1987). As the level of dUMP rises, a subsequent rise in the level of dUTP is likely (Aherne, Hardcastle et al. 1996). Both dUTP and FdUTP can be misincorporated into DNA, causing DNA-damage. The base excision repair system will attempt to repair the damage, but the high levels of dUTP and FdUTP compared to the low level of dTTP increase the chance that dUTP or FdUTP will be reincorporated, and a futile cycle of misincorporations will eventually lead to DNA strand breaks, loss of replication fork stability and cell cycle arrest (Aherne, Hardcastle et al. 1996; Kouzminova and Kuzminov 2006).

1.2.2 Methyl methanesulfonate

Methyl methanesulfonate (MMS) is a DNA-alkylating agent, but its mechanism is less understood than 5FU. It predominantly methylates guanine residues at the N-7 position, but other methylations can occur as well, as shown in Figure 1-6.

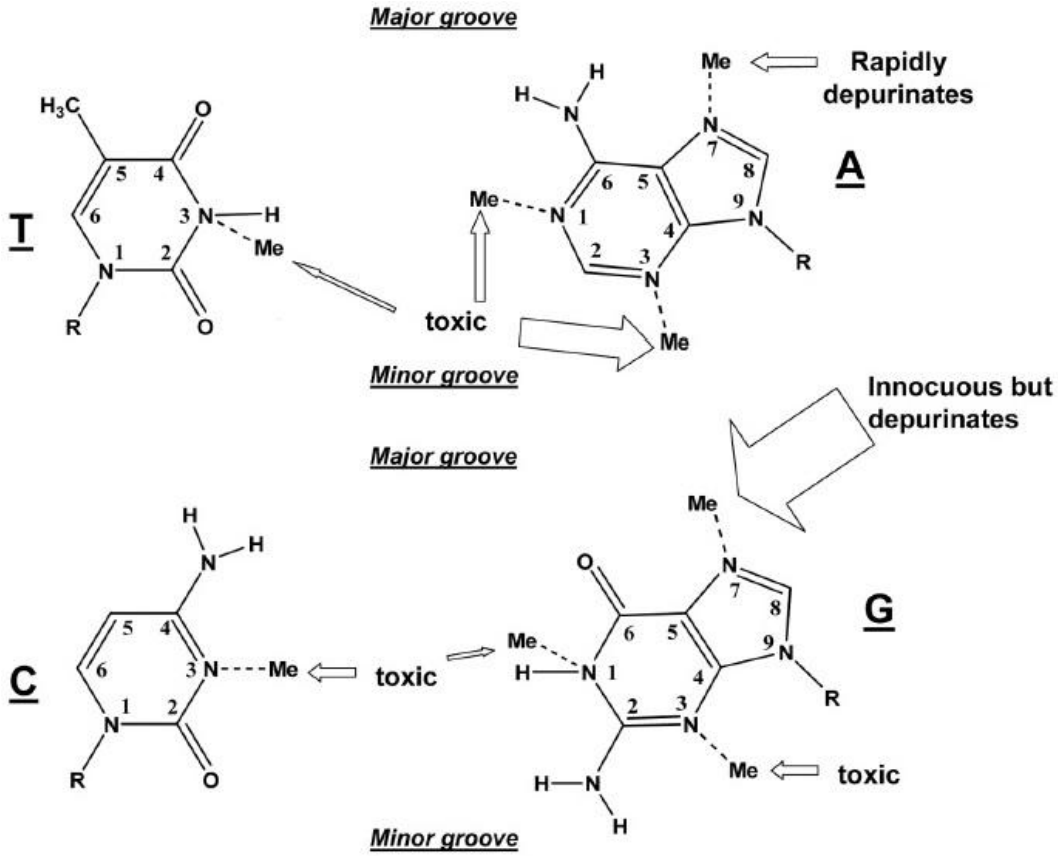

Figure 1-6: Possible sites for methylation in double stranded DNA (Adapted from Wyatt and Pittman 2006). The size of the arrows indicate the relative proportion of adducts, and their effects of the methylations are stated. Methylation of different sites on the same base is extremely rare. T: thymine, A: adenine, C: cytosine, G: guanine.

Methylation of the N7-position in guanine leads to depurination, which produces an abasic site that can have mutagenic and toxic effects on the cell (Wyatt and Pittman 2006). Methylation of the N1-position of adenine and the N3-position of cytosine are toxic and can produce some mutagenesis (Dinglay, Trewick et al. 2000), and they can also block replication of DNA (Delaney and Essigmann 2004). Methylations of guanine at the N1-position and of thymine at the N3-position have also been shown to block replication and be mutagenic (Delaney and Essigmann 2004).

1.3 Metabolomics

In order to sustain vital functions such as growth and reproduction, maintenance of cell structures and responding to environmental changes, there is a multitude of chemical reactions in the cells of an organism occurring at any given time. The building of components in a cell is called *anabolism* while the breaking down of components is called *catabolism*. The complete set of anabolic and catabolic reactions is called the *metabolism* of the cell. The small substances involved in the metabolism, intermediates and products, are called *metabolites*, and the complete set of metabolites in an organism is called the *metabolome*. Metabolomics is the study and analysis of the metabolome. The range of metabolites is wide, and includes sugars, fatty acids, and amino acids.

The information gathered from metabolomics can be used in different ways. Studies of a single metabolite in different phases of fermentation can reveal effects that are limiting or inhibiting metabolism, or give new information about active metabolic pathways in the organism being studied (Buchholz, Hurlebaus et al. 2002).

The most common methods for metabolite detection are nuclear magnetic resonance spectroscopy (NMR), liquid chromatography – mass spectrometry (LC – MS) and gas chromatography – mass spectrometry (GC – MS). Which method to use is dependent on the metabolites to be analyzed, as each method has its strengths and weaknesses.

NMR utilizes the magnetic properties of atomic nuclei to determine physical and chemical properties of molecules in a sample, and can be used to directly investigate samples without significant sample preparation. It is a fast and highly quantitative method widely used in epidemiology studies of high abundance metabolites in very large population studies (Solomon and Fischer 2010). NMR used to be the prevalent method for metabolite analysis, but has the last 10-15 years been surpassed by GC – MS and LC – MS, due to being several orders of magnitude less sensitive. NMR is now used more as a complementary tool to the other two methods as NMR can discriminate positional and structural isomers, and provide the information needed to give a *de novo* characterization of chemical structures (Solomon and Fischer 2010).

GC - MS combines the features of gas chromatography (GC) and mass spectrometry (MS) to provide an accurate way of identifying substances that may not be possible using either of these methods separately. It requires the analyte to be vaporized in order to migrate through the capillary, and is therefore limited to molecules that are volatile or amenable to chemical

derivatization that renders them volatile (McMaster 2008), effectively creating some upper weight limits.

LC – MS combines the physical separation of molecules in liquid chromatography with the mass analysis in mass spectrometry. It can detect a broader range of molecules than GC – MS since it does not require the analytes to be volatile nor derivatized and it is the preferred method of choice for un-targeted metabolomics studies (Solomon and Fischer 2010) or discovery-based research of unknown metabolites (Agilent Technologies Inc. 2007). One major disadvantage it has to GC – MS is a substantially higher investment cost (Agilent Technologies Inc. 2007).

Figure 1-7 shows which method is best suited for analyzing different compounds. The method of choice depends on the physical and chemical properties of the molecules.

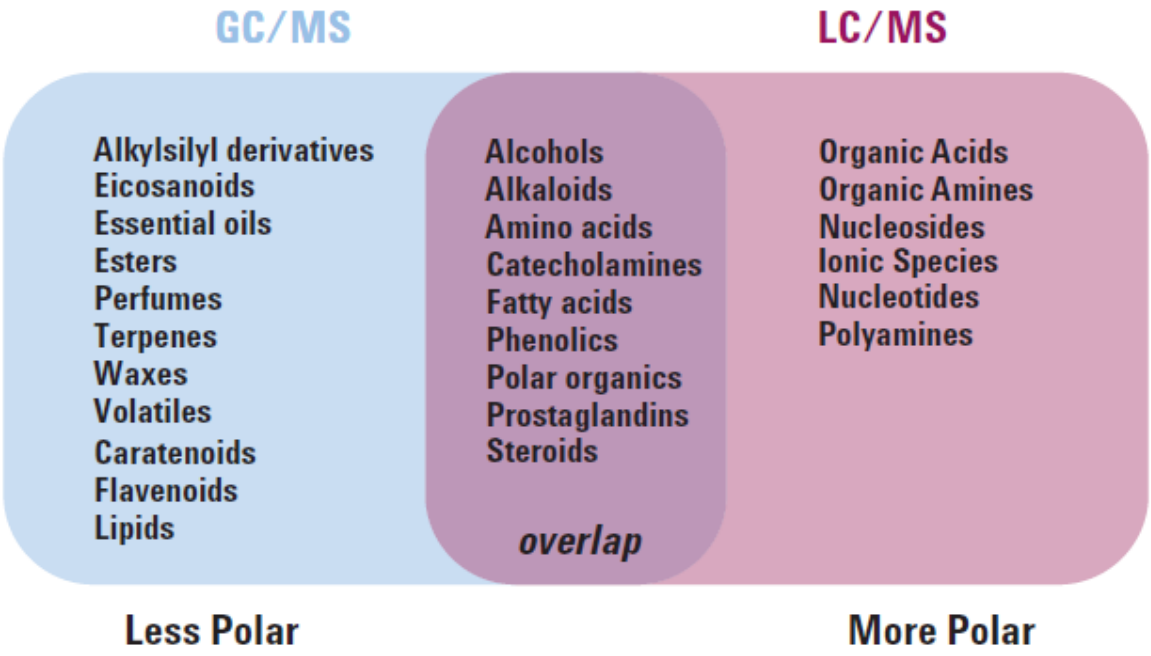

Figure 1-7: Classes of chemicals and the analytical techniques with which they are most compatible (Agilent Technologies Inc. 2007).

The method used in the work for this thesis was GC – MS single quadrupole, described in detail in the next section.

1.4 Gas Chromatography - Mass Spectrometry

A model of a typical GC - MS system is shown in Figure 1-8.

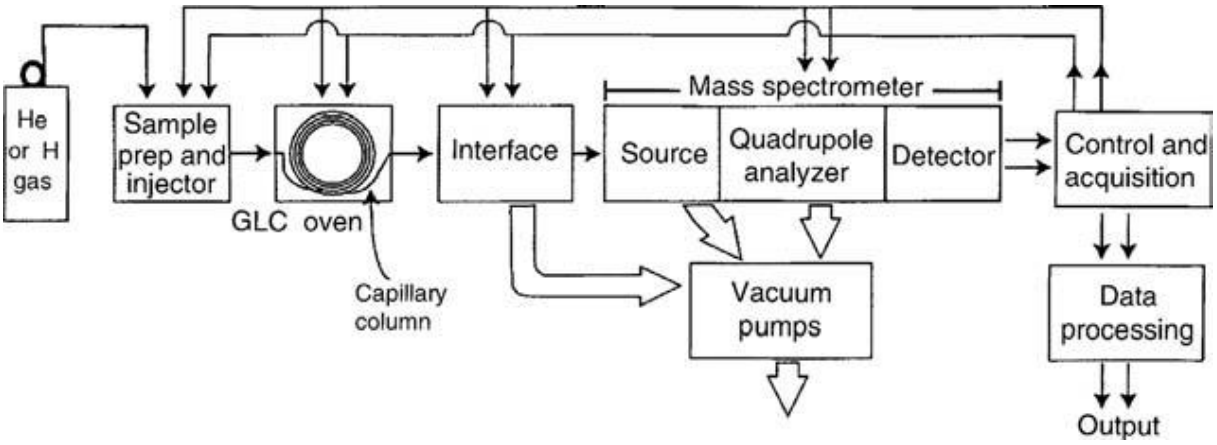

Figure 1-8: Diagram of a typical GC - MS system (McMaster 2008).

The liquid sample to be analyzed is injected into the injector of the GC where it is evaporated. The evaporated sample is transported through the heated separation column by an inert carrier gas (Helium). The column is a coiled capillary tube coated with a stationary phase, allowing gas-liquid separation to take place. Most stationary phases are thermally stable polymers of a high molecular weight, present either as liquids or as gums. The most common types of stationary phases are the polysiloxanes and polyethylene glycols (Grob and Barry 2008). Each material has different chemical properties, allowing optimization of the separation depending on the type of compound to be analyzed. The components of the analyte are separated due to absorptive interactions with the coating as they pass through the column. The time it takes for a component to exit the column is referred to as the retention time (RT) of the component. A limitation when analyzing with a chromatograph alone is that different compounds might have very similar retention times, which can be a challenge when using this method for identification.

As the separated components exit the column of the GC, they are transferred to the mass spectrometer. As they enter the MS part of the system, the components are ionized in a high vacuum. Ionization can occur in several different ways: Electron Ionization (EI), Chemical Ionization (CI), Fast Atom Bombardment, or Field Ionization (FI). The most common method is EI (McMaster 2008), which was also the method used in this work. In EI a stream of electrons with energy of 70 eV collides with the molecules eluting from the GC column. This collision causes an electron to be knocked off the sample molecule, creating a positively ionized molecule. The sample molecule is also fragmented in the process, and the

fragmentation pattern created is characteristic for the ionized molecule for a given electron energy, making differentiation between different compounds possible. Unknown analytes can be screened against a library of retention times and/or fragmentation patterns for known compounds, and the composition of the sample can be determined.

After fragmentation, the ionized molecule and the fragments are guided into a quadrupole analyzer (Figure 1-9).

Figure 1-9: The 4 cylindrical rods of a quadrupole mass analyzer (Worley and Kvech 1999).

The quadrupole consists of 4 cylindrical rods made of quartz. A direct current (dc) and a radio frequency oscillator (RF) are applied on the quadrupole, each rod having opposite charge of the adjacent rods (and the same charge as the opposite rod). This causes the stream of fragments and ions to follow a helical, sine wave path through the quadrupole. As the dc/RF field sweeps higher or lower, it disturbs this path for all but one of the single-mass fragments. While the disturbed fragments collide with the walls of the quadrupole, this single-mass fragment safely continues through the quadrupole and on to the ion detector.

Results from analysis done by MS alone can be difficult to interpret, as a mixture of components can result in a large amount of fragments and ions with similar mass/charge ratio. Separating compounds in the GC column before analysis with the MS makes it easier to quantify single compounds in a complex mixture as there are fewer fragments to consider at any time.

1.4.1 Sample preparation

As previously mentioned, not all compounds are amenable to direct analysis with GC - MS due to low volatility or stability. Derivatization is a method used to increase the volatility of a compound by chemically modifying it, creating a derivative of the original compound. The new properties of the modified compound make it amenable to chromatographic separation. Smaller molecules with polar groups have a low volatility, as there are strong attractive forces between them. Polar molecules can also adsorb on the active surfaces inside the column walls, which leads to a decrease in volatility. Derivatization increases volatility by addition of non-polar groups to the polar groups, thus eliminating these effects. Other advantages of derivatization include improved selectivity, chromatographic efficiency, and enhanced detectability (Regis Technologies Inc. 2008). Different methods of derivatization are named after the group that is transferred to the sample molecules. Silylation is the addition of a silyl group, alkylation is the addition of an alkyl group, and acylation is the addition of an acyl group. The most prevalent method is silylation (Regis Technologies Inc. 2008), which was the method used for this work.

The derivatization agent used was *N*-(*tert*-butyldimethylsilyl)-*N*-methyl-trifluoroacetamide (MTBSTFA), its molecular structure is shown in Figure 1-10.

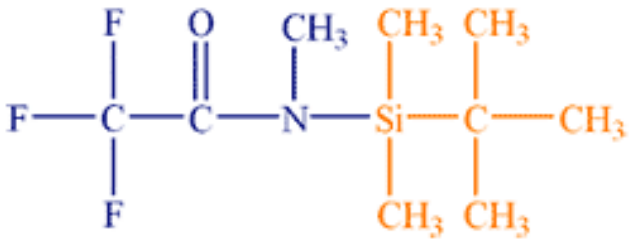

Figure 1-10: The molecular structure of *N*-(*tert*-butyldimethylsilyl)-*N*-methyl-trifluoroacetamide. The silylating group, *t*-butyl-dimethylsilyl, is shown in orange (Campbell Science 2011).

This is a silylating agent that replaces active hydrogens on the sample molecule with a *tert*-butyldimethylsilyl (*t*-BDMS) group. When this derivative of the sample molecule is inserted into the mass spectrometer, it is ionized and split into fragments. Depending on which bonds are broken, different fragments are produced. For *t*-BDMS derivatives of amino acids there are 5 possible outcomes of fragmentation, shown in Figure 1-11.

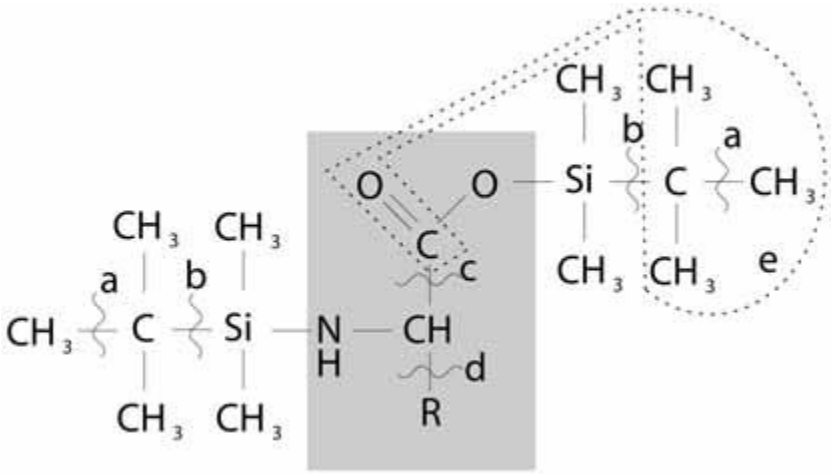

Figure 1-11: The possible fragments of amino acids derivatized with MTBSTFA when ionized in a mass spectrometer. (a) M-15 and methyl group; (b) M-57 and *tert*-butyl group; (c) M-159 and C(O)O-*t*-DBMS ion; (d) f302 and the side chain of the amino acid; (e) M-85 and the CO of the amino acid and a *tert*-butyl group (Nanchen, Fuhrer et al. 2007).

1.4.2 Interpreting results from GC - MS

The data obtained from GC - MS are given as a three-dimensional block, the coordinates being elapsed time, mass/charge ratio (*m*/*z*) and ion concentration (Figure 1-12).

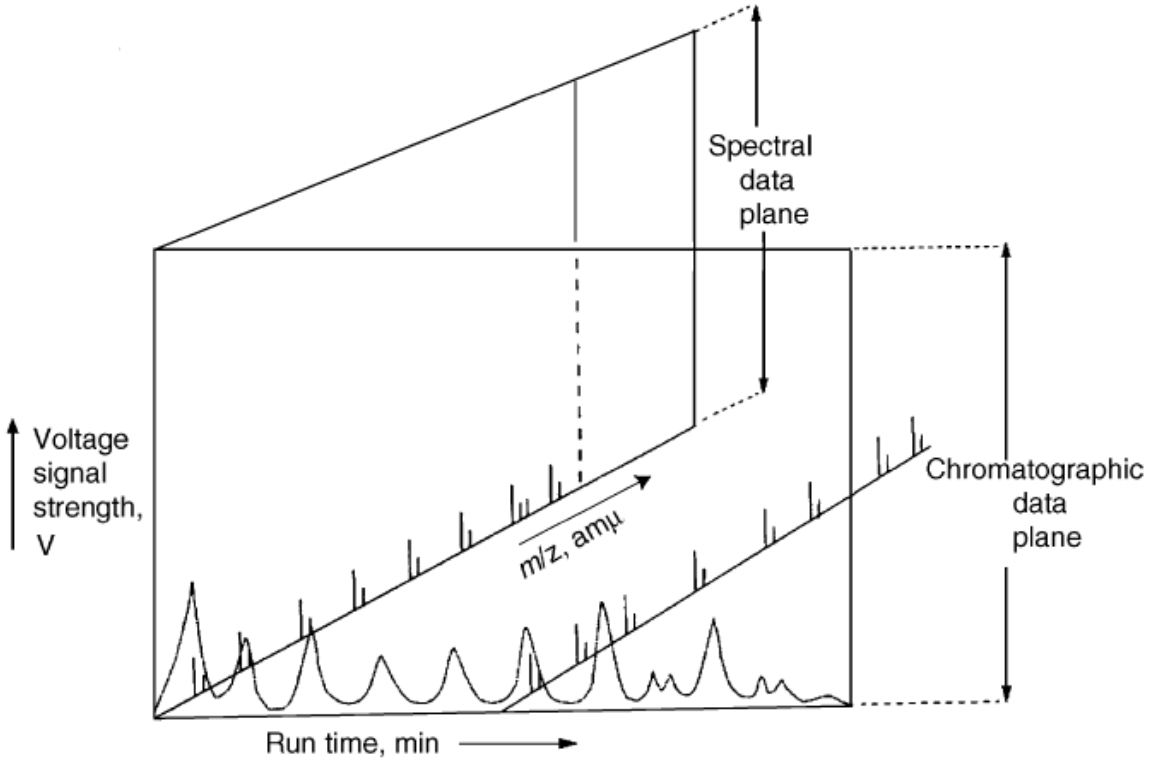

Figure 1-12: The three-dimensional data block obtained from analysis with GC/MS (McMaster 2008).

This three dimensional block of data is impractical when it comes to analyzing a sample, as the amount of information can be overwhelming for even the most experienced scientist. The data are more easily interpreted when presented with only two dimensions, and this can lead to a variety of ways of presenting the data.

The simplest output from the GC – MS is the total-ion chromatogram (TIC). It summarizes the signal strengths of all ions detected by the MS at any given time (Figure 1-13).

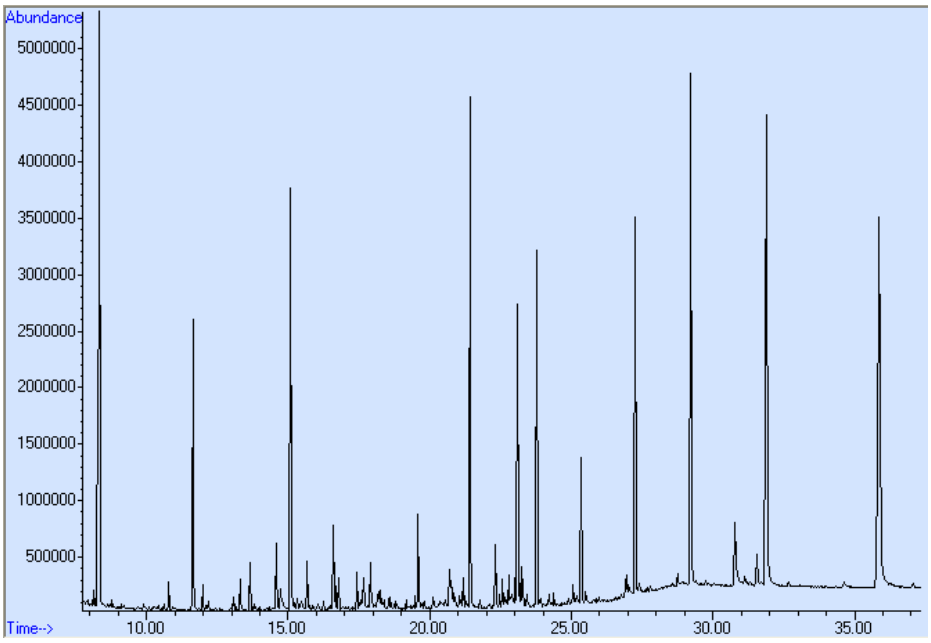

Figure 1-13: A total-ion chromatogram for a sample taken from a culture of *S. cerevisiae* stressed with NaCl.

This provides an overview of the retention times of the analytes, as each peak represents the set of fragments that is detected by the MS belonging to the compound that elutes from the GC. Due to overlap of eluting compounds, the TIC has a limited use as a single peak may consist of several different compounds.

An extracted-ion chromatogram (EIC) selects all data for a single molecular ion mass and a plot of the concentration of the ions of the selected mass versus time is produced (Figure 1-14).

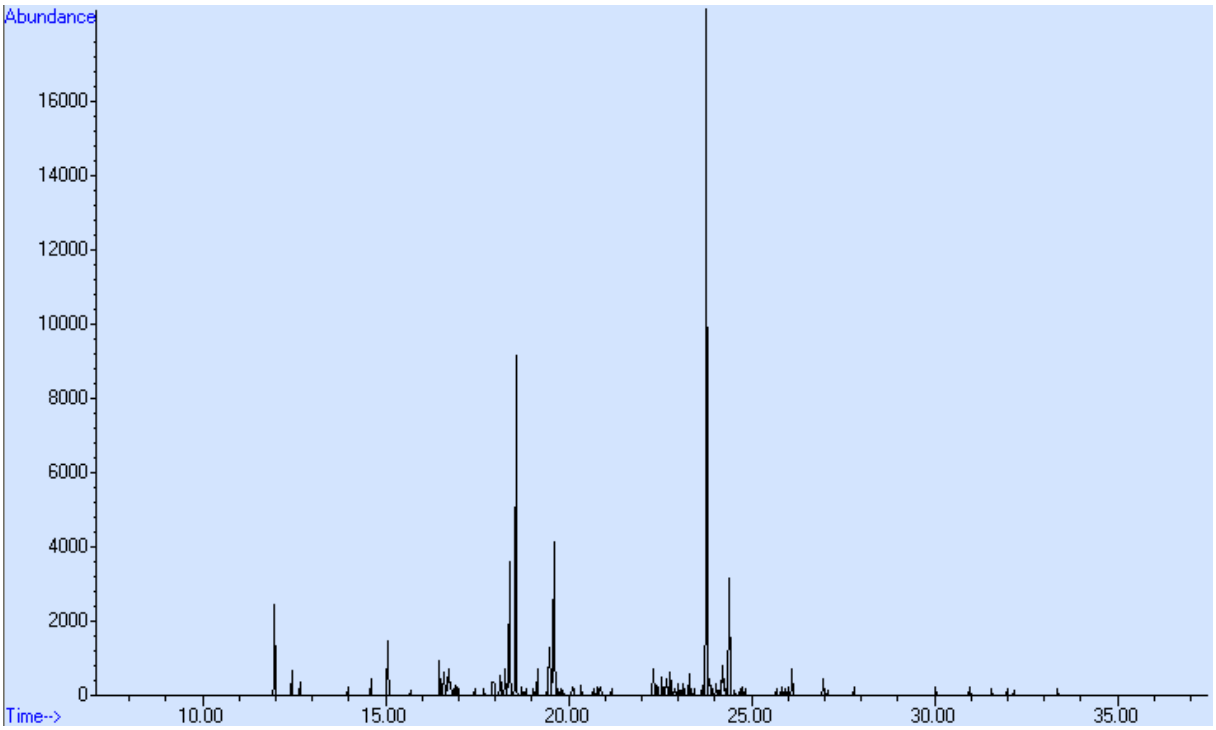

Figure 1-14: Extracted ion chromatogram for all ions with m/z of 288, sample taken from a culture of *S.cerevisiae* stressed with NaCl.

The peaks in this chromatogram represent the concentration of ions of a selected molecular mass as they appear during the chromatographic run. This allows for a more selective representation, especially useful for differentiation of co-eluting compounds with dissimilar fragmentation patterns.

Another useful approach is to look at the total mass spectrum at a given time. The mass spectrum of threonine is shown in Figure 1-15. The specific time is 18.515 minutes, the time it takes for MTBSTFA-derivatized threonine to pass through the column of the GC and enter the MS.

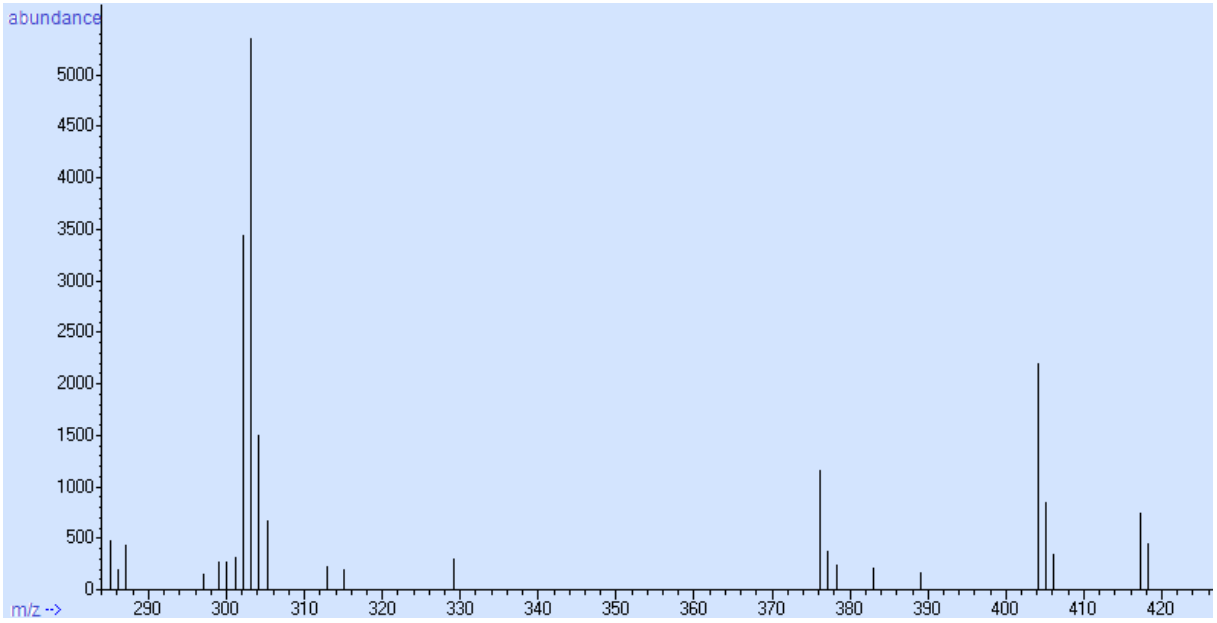

Figure 1-15: The fragmentation pattern of MTBSTFA-derivatized threonine, eluting at 18.515 minutes.

Some variations in the fragmentation pattern or ion concentration can occur due to changes in geometry, calibration, cleanliness, and ion detector age (McMaster 2008), and controlling these is vital to ensure reproducible data.

When performing analysis with GC – MS there is a risk that a chromatographic peak may be a composite of overlapping components due to incomplete chromatographic separation. This can make it difficult to determine which spectral data belongs to which compound. To overcome this, a Deconvolution Reporting Software (DRS) has been developed that can separate overlapping mass spectra into spectra of the individual components (Solomon and Fischer 2010). The term deconvolution is "used here in the broad sense of extracting one signal from a complex mixture. The treatment of noise, the correction for base line drift, and the extraction of closely co-eluting peaks from one another is all part of the deconvolution process " (Agilent Technologies Inc. 2011). The process is illustrated in Figure 1-16.

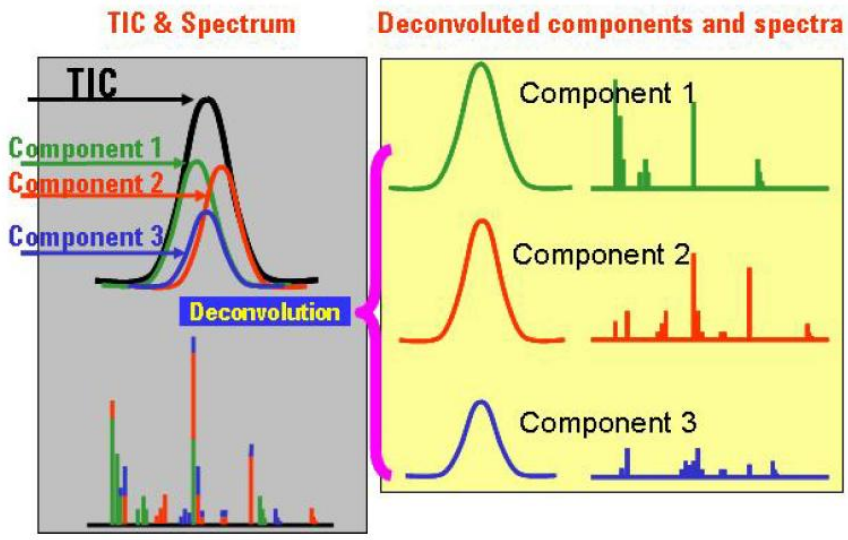

Figure 1-16: Illustration of the deconvolution process by DRS (Solomon and Fischer 2010).

DRS combines results from three softwares; Agilent MSD Productivity Chemstation, the National Institute of Standards and Technology (NIST) Automated Mass Spectral Deconvolution and Identification Software (AMDIS), and the NIST 2008 Mass Spectral Search Program (NIST08) to create a single target compound analysis report (Agilent Technologies Inc. 2011). The data provided can either be compared to the NIST compound library, containing more than 190 000 mass spectra, or the user can create a custom library using data obtained from analysis of a selection of known compounds.

1.5 Fluxomics

As molecules are processed through a metabolic or transporting pathway they create a flux, much like electrons in an electric current. The array of all fluxes for all reactions in an organism is referred to as the *fluxome* (Sauer, Lasko et al. 1999). Fluxomics can be defined as the discipline that analyzes the fluxome as one part of systems biology (Bornholdt 2005), or as the quantification of the intracellular metabolite turnover rates in a cell (Feng, Page et al. 2010). Fluxome analysis has in recent years become a useful tool for increasing our understanding of a wide range of organisms, from bacteria and unicellular eukaryotes to animals, plant cells and whole organs (Wiechert, Schweissgut et al. 2007). Examples of its applications are monitoring of different growth phases (Wahl, El Massaoudi et al. 2004), diagnosis of the effect of genetic manipulations (Emmerling, Dauner et al. 2002) and the effect of different physiological conditions on an organism (Kiefer, Heinzle et al. 2004).

The currently most used fluxomics technology is ^{13}C metabolic flux analysis (^{13}C-MFA), where the organism is fed with substrates labeled with carbon-13. A typical substrate is a

mixture of 80 - 90 % natural-abundance glucose and 10 – 20 % [U-$^{13}C_6$] glucose (Sauer, Lasko et al. 1999). Depending on the metabolic reactions, the carbon-carbon bonds are cleaved and formed to create randomly labeled isotopes of metabolites. These isotopes will create unique fragments that can be detected by mass spectrometry, and the flux ratios can be determined by probabilistic equations that relate the intensities of the multiplet components to the relative abundance of the intact carbon fragments (Szyperski 1995).

1.6 FiatFlux 1.6X

As fluxomics is a new field of research, a part of the work for this thesis was to explore methods for obtaining useful data in the study of the fluxome of yeast. Protocols for growing cells on media containing ^{13}C-glucose exist in the literature, but interpretation of the data obtained can be a challenge. Calculation of the intracellular fluxes is a highly complex task, not easily performed by non-experts of the field. The calculations require large and heterogeneous data sets, obtained from highly controlled experimental conditions, which limited the research of intracellular fluxes to a few expert groups. The publicly available software FiatFlux 1.6X was developed to assist with these calculations, opening this field of research to a wider group of scientists (Zamboni, Fischer et al. 2005).

FiatFlux uses raw MS data to perform metabolic flux analysis. It is preconfigured to process amino acids derivatized with MTBSTFA and analyzed with an EI ionizing GC - MS, and it can model three different organisms, *Escherichia coli*, *Bacillus subtilis* and *S. cerevisiae*. The program has two main operating modules; RATIO which calculates metabolic flux ratios from raw MS-data, and NETTO which estimates the net carbon fluxes.

In the RATIO module, FiatFlux will generate a matrix containing the total ion count for each timepoint and the considered m/z value (Zamboni, Fischer et al. 2005). Each recognized analyte will give a mass isotopomer distribution vector MDV_α extracted from this matrix,

$$MDV_\alpha = \begin{bmatrix} m_0 \\ m_1 \\ \vdots \\ m_n \end{bmatrix} \text{ with } \sum m_i = 1 \qquad (1.1)$$

where m_0 is the fractional abundance of molecules with monoisotopic mass and $m_{i>0}$ is the abundance of the heavier mass fragments. To obtain the mass isotope distribution vector for a specific carbon backbone (MDV_A), MDV_α is corrected for naturally occurring isotopes of O,

N, H, P, S, Si and C atoms in the derivatized agent (van Winden, Wittmann et al. 2002), and for the presence of unlabeled biomass in the sample, originating from the inoculum (Fischer and Sauer 2003). These MDV_{α} are in turn used to estimate the mass distribution vector of their precursors (MDV_M) by least square fitting. The flux ratios are then calculated from MDV_M with probabilistic equations, including standard deviations (Fischer and Sauer 2003).

In the NETTO module, metabolite balances and flux ratios are used to construct a system of constrains (Zamboni 2007). One example is the ratio of pyruvate originating from malate. The upper bound (c) can be defined as

$$c \geq \frac{v_{mae}}{v_{mae} + v_{pyk}} \tag{1.2}$$

where v_{mae} is the flux through the malic enzyme and v_{pyk} is the flux through pyruvate kinase. A restriction can be derived from this definition

$$(1-c) \cdot v_{mae} - c \cdot v_{pyk} \leq 0 \tag{1.3}$$

Similar constrains can be derived for a series of fluxes. The constraints are transformed to matrix notation, with the formation of biomass added as a reaction that withdraws precursors. The following system of equations can be used to calculate the net carbon fluxes:

$$\begin{cases} A_{EQ} \cdot \begin{bmatrix} v_1 \\ \vdots \\ v_n \\ -\mu \end{bmatrix} = b_{EQ} \\ A_{BND} \cdot \begin{bmatrix} v_1 \\ \vdots \\ v_n \\ -\mu \end{bmatrix} \leq b_{BND} \end{cases} \quad \text{with } A_{EQ}^{\{m+p \times n+1\}} = \begin{bmatrix} s_{1,1} & \cdots & s_{1,n} & bm_1 \\ \vdots & \ddots & \vdots & \vdots \\ s_{m,1} & \cdots & s_{m,n} & bm_m \\ r_{1,1} & \cdots & r_{1,n} & 0 \\ \vdots & \ddots & \vdots & \vdots \\ r_{p,1} & \cdots & r_{p,n} & 0 \end{bmatrix}, b_{EQ}^{\{m+p \times 1\}} = \begin{bmatrix} b_1 \\ \vdots \\ b_m \\ 0 \\ \vdots \\ 0 \end{bmatrix}, \tag{1.4}$$

$$A_{BND}^{\{q \times n+1\}} = \begin{bmatrix} r_{p+1,1} & \cdots & r_{p+1,n} & 0 \\ \vdots & \ddots & \vdots & \vdots \\ r_{p+q,1} & \cdots & r_{p+q,n} & 0 \end{bmatrix}, b_{BND}^{\{q \times 1\}} = \begin{bmatrix} 0 \\ \vdots \\ 0 \end{bmatrix}$$

The system has m metabolites, n reactions, p constraints derived from equality reaction ratios, and q constraints from upper or lower reaction bounds. $S_{i,j}$ is the stoichiometric factor of metabolite i in reaction j, bm_i is the biosynthetic demand for metabolite i, $r_{k,j}$ is a scalar that

depends on flux ratio k and describes its relation to reaction j, v_i is the flux through reaction i to be estimated, μ is the growth rate, and b_j is the measured net production rate of metabolite j. b_j is negative for substrates.

By solving this system of linear constraints, the net fluxes can be calculated. Two outcomes are possible, an underdetermined system without a unique solution but with a solution space with an infinite number of flux distributions, or a determined or overly constrained system where the flux distribution is calculated by least square iterative fitting .

The operating window of FiatFlux 1.6X is shown in Figure 1-17.

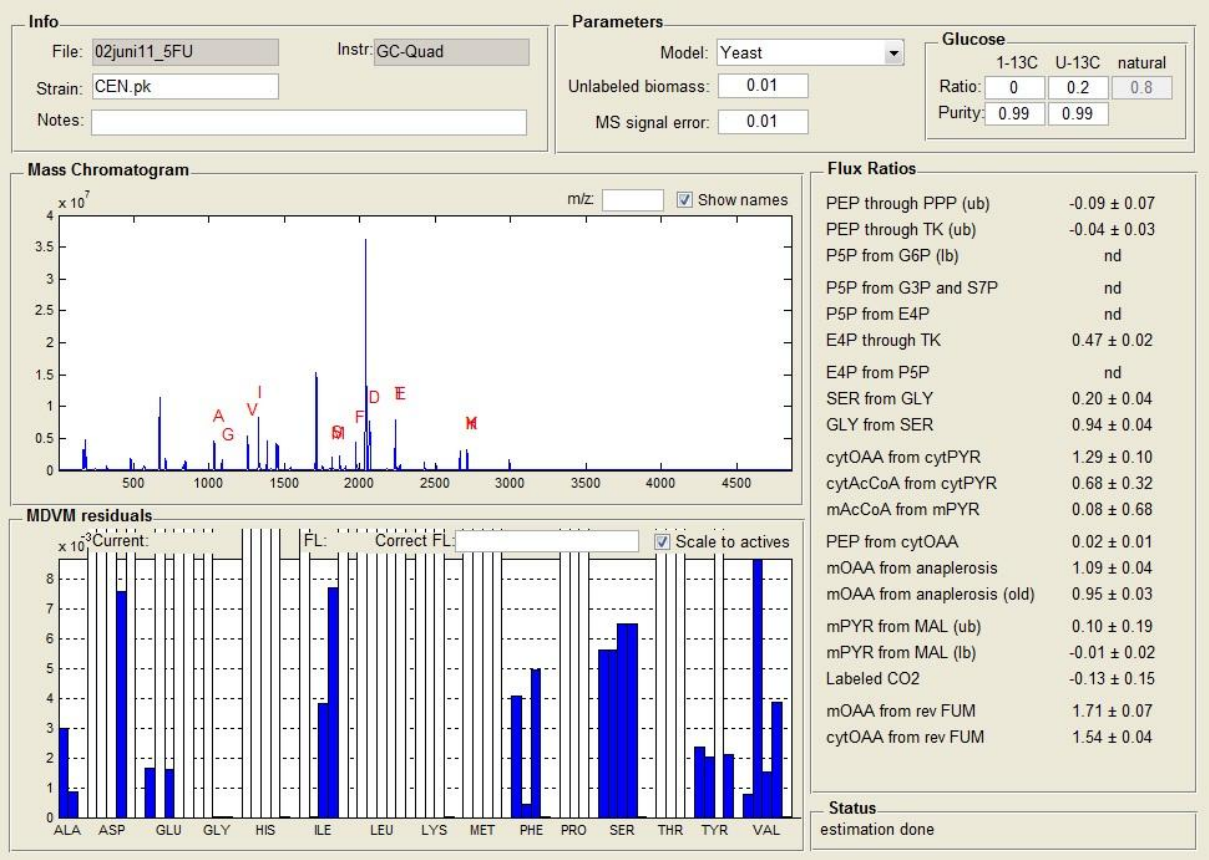

Figure 1-17: The main operating window of FiatFlux 1.6X. The *Info* panel contains general information about the analyzed sample. The *Paramaters* panel lets the user define the experimental parameters. The *Mass Chromatogram* panel shows the TIC of the sample or, if an m/z value is entered, the corresponding EIC. The *MDVM residuals* panel shows the residuals of the MDV_M fitting procedure. The *Flux Ratios* panel shows the calculated flux ratios, "nd" indicating that a flux could not be determined.

The calculation of flux ratios is based on the fragments of the analytes, and the quality of these fragments must be considered to ensure the validity of the calculated flux ratios. In FiatFlux the user has the option of excluding fragments that exhibit a troublesome MDV_A, and this can be assessed in different ways. MDV_M residuals higher than 10^{-2} are "of dubious quality" (Zamboni 2007), and exclusion of such residuals should be considered. The fractional labeling (FL) of metabolites and products should reflect that of the substrate (80 % naturally labeled glucose and 20 % [U-^{13}C glucose] gives a FL of 0.20), and all fragments that does not have FL between 0.17 and 0.23 should be excluded. This can be done in the weight fitting window (Figure 1-18).

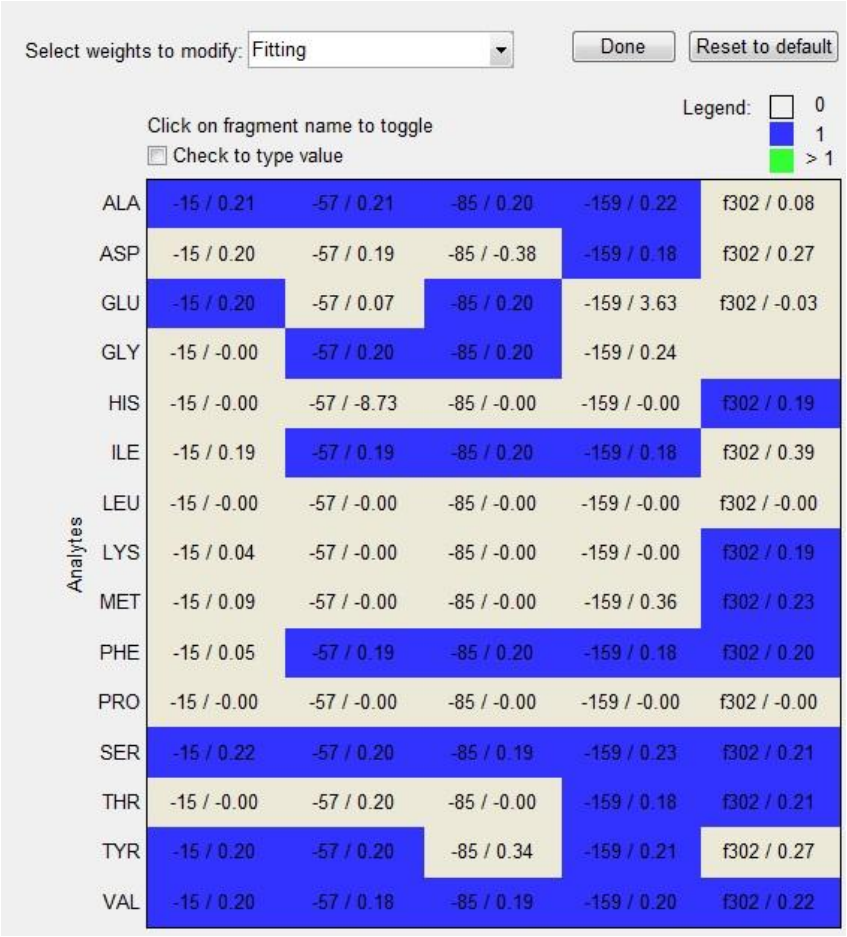

Figure 1-18: Weight fitting window of FiatFlux. The fragments of the analytes are shown as "Fragment name"/"Fractional labeling". Fragments in blue are given a weight of 1; uncolored fragments are given a value of 0.

1.7 Aim for this master thesis

The main goal for this master thesis was to investigate the metabolic response of *S. cerevisiae* to DNA damaging agents.

An experimental platform was to be established for studying the change in the metabolome of a culture of *S. cerevisiae* as 5FU was added during the exponential growth phase. A protocol for GC – MS analysis, using MTBSTFA as the derivatizing agent, was to be implemented and used to create a custom DRS library. The library was to contain data for a selection of metabolites found in *S. cerevisiae*, mainly amino acids but also some of the metabolites from the TCA cycle. The microorganism was to be grown under controlled conditions in a bioreactor, and samples taken as DNA damaging compounds were added to the culture during its exponential growth phase. The samples would then be analyzed using the newly created DRS library, and changes in the metabolome as a response to the DNA damage could be determined.

A similar experimental platform was also to be established for metabolic flux studies, by cultivating *S. cerevisiae* in medium containing labeled [U-^{13}C]-glucose and in the presence of the DNA damaging compounds 5FU or MMS. The metabolic fluxes were then to be calculated using FiatFlux 1.6X and compared to the fluxes of an unstressed culture.

2 Materials and methods

2.1 Strains of S. cerevisiae

The laboratory strain *S. cerevisiae* CEN.pk was used for all experiments. This family of strains was originally constructed with the specific requirements of physiologists, geneticists, and engineers in mind. It is a result of a series of crosses and backcrosses of two laboratory strains, which eventually lead to final strain with properties well suited for laboratorial experiments (van Dijken, Bauer et al. 2000).

2.2 Cultivation of *S. cerevisiae*

2.2.1 Media and solutions

Rich medium

5.0 g/L yeast extract (OXOID, 1014708)

20 g/L Soyton Peptone (DIFO, FK0417XC)

The ingredients were dissolved in water and the solution was autoclaved at 120 °C for 20 minutes.

Mineral medium

5 g/L $(NH_4)_2SO_4$ (Merck, LOT A801717705)

3 g/L KH_2PO_4 (Merck, LOT A672173637)

The ingredients were dissolved in ion-free water, pH adjusted to 5 with NaOH and the solution was autoclaved at 120 °C for 20 minutes. For experiments in shake flasks, 100 mM of potassium hydrogen phthalate was added as a buffer to avoid changes in pH.

Trace elements solution

0.30 g/L $FeSO_4*7H_2O$ (Merck, LOT 1173391)

0.45 g/L $ZnSO_4*7H_2O$ (Merck)

0.228 g/L $CaCl_2$ (Merck, LOT F356083 802)

0.08 g/L $MnCl_2*7H_2O$ (Merck, LOT 9657938)

0.03 g/L $CoCl_2*6H_2O$ (Reagenzien Merck, LOT 8489035)

0.4 g/L $Na_2MoO_4*2H_2O$ (Sigma Chemical Company)

1 g/L H_3BO_3 (Sigma Chemical Company)

0.03 g/L $CuSO_4*5H_2O$ (Acros Organics, LOT A014205301)

0.01 g/L KI (Merck, LOT B158343 234)

1.3 g/L EDTA (Sigma Chemical Company, LOT 61F-0318)

The ingredients were dissolved in ion-free water, the pH adjusted to 4.0 and the solution was filter-sterilized.

Vitamin solution

28.6 mg d-biotin was dissolved in 10 mL 0.1 M NaOH, 400 mL of distilled water was added and pH was adjusted to 6.5 with HCl.

The following vitamins were then added:

500 mg Ca-Panthothenate (Merck, LOT 251637 art: 2316)

500 mg Thiamin-HCl (Acros Organics, LOT A016611101)

500 mg Pyridoxine-HCl (Sigma Chemical Company, LOT 76F-0367, No. P-9755)

500 mg Nicotinic acid (Sigma Chemical Company, LOT 51C-1670, No. N-4126)

100 mg p-aminobenzoic acid (Sigma Chemical Company)

pH was adjusted to 6.5, and 12 g m-inositol (Sigma Chemical Company, No. I-5125) was added before pH was readjusted to 6.5. Ion-free water was added to a final volume of 500 mL and filter-sterilized.

Glucose solution

A glucose solution of concentration of 200 g/L was made by dissolving 50 g glucose (AnalaR Normapur, LOT 07E070003) in 250 ml ion-free water. The solution was autoclaved at 120 °C for 20 minutes.

Magnesium sulfate solution

50 g/L $MgSO_4$ (Sigma Chemical Company)

$MgSO_4$ was dissolved in ion-free water and autoclaved at 120 °C for 20 minutes.

Yeast minimal medium

The yeast minimal medium (Verduyn, Postma et al. 1992) was prepared by mixing the previously described solutions.

For cultivations in the bioreactor, the following amounts were added to 700 ml of mineral medium:

0.77 ml of trace elements solution

7.7 ml of magnesium sulfate solution

1.54 ml of vitamin solution

For experiments in shake flasks, the following amounts were added to 100 ml mineral medium:

110 µl of trace elements solution

1.1 ml of magnesium sulfate solution

220 µl of vitamin solution

Glucose solution was added as needed to obtain the desired glucose concentrations.

2.2.2 Cultivation of cells

Cultivations in shake flasks were done in 250 or 500 ml baffled, Erlenmeyer flasks containing 25 or 100 ml of medium, respectively. The cells were grown in an Infors HT Minitron AG CH-4103 BOTTMINGEN shaking incubator at 30 °C and 225 rpm.

Cultivation of cells in a bioreactor was done in a 1.3 liter BioFlo®/CelliGen® 115 Benchtop Fermentor & Bioreactor from New Brunswick Scientific with 700 ml of medium. Inoculum was prepared by inoculating 100 µl of freeze stock of *S. cerevisiae* CEN.pk in a shake flask with 100 ml rich medium, and growing overnight. 20-50 ml of the overnight culture was centrifuged for 5 minutes at 5000 rpm and the supernatant removed. The cell pellet was dissolved in 5 ml medium and transferred to the bioreactor. The cultivation was carried out at

30 °C, pH=5 and airflow of 0.5 vvm. The dissolved oxygen was kept at 40% by stirring. Stirring speed was set at a minimum of 50 rpm and a maximum of 1000 rpm. To monitor the O_2 and CO_2 levels of the outgoing airflow a Rosemount Analytical X-STREAM XE process gas analyzer was used.

2.2.3 Optical density measurements

Optical density (OD) measurements were done with a Pharmacia Biotech Ultrospec 2000 UV/Visible Spectrophotometer. The wave length was set to 600 nanometers, and a solution of 1.5 wt% NaCl was used to as zero reference. All measurements were done within OD_{600} values between 0 and 0.7. Samples that gave values above this threshold were diluted with 1.5 wt% NaCl solution, and the OD_{600} was calculated accordingly.

2.2.4 Sampling from the bioreactor and boiling ethanol extraction

A previous study has compared methods for extracting intracellular metabolites and concluded that boiling ethanol extraction gives almost 100 % recovery and good reproducibility (Canelas, ten Pierick et al. 2009), and the boiling ethanol protocol used for this work was adapted from this method.

Samples of 8 ml culture were transferred to a 0.8 µm Millipore filter under vacuum pressure and allowed to flow through completely. The filter and sample were washed twice with 8 ml of 2.63 wt% NaCl solution under vacuum pressure. The washed filter was transferred to a tube containing 8 ml of 75% ethanol and preheated to 95 °C. 100 µl of 1 mM internal standard of d3-alanine was added and the tube was kept at 95 °C in a water bath for 3 minutes. The tubes were then transferred to a cryostat (-40 °C). To separate the cell walls from the supernatant, the sample was centrifuged at room temperature for 5 minutes at 5000 rpm. Prior to centrifuging the filter was removed from the tube with sterile tweezers. After centrifuging, 3x2 ml of the supernatant was transferred using a pipette to new sterile tubes without disturbing the precipitate. The samples were dried using a Thermo SPD2010 Integrated SpeedVac System for 3-5 hours (until all liquid has evaporated), 60 °C, 5.1 Torr and stored at -80 °C until further use.

2.2.5 Sampling from shake flasks

Aliquots of 1.5 ml of culture were transferred to 2.0 ml eppendorf tubes. The cells were centrifuged at 14.000 rpm for 5 minutes, and the supernatant was discarded. The cells were washed with 1.5 ml of mineral medium, centrifuged and the supernatant was discarded. The

cells were hydrolyzed in 500 µl 6M HCl for 24 hours at 105 °C, and dried on a heating block under a constant stream of N_2. The samples were stored at -80 °C until further use.

2.2.6 Sample preparation for GC-MS analysis

The sample to be analyzed by GC - MS was dissolved in 100 µl of pyridine. 50 µl of the dissolved sample was transferred to an injection vial containing an insert, 70 µl of MTBSTFA was added and the mixture was thoroughly mixed. The mixture was heated at 60 °C for 30 minutes and allowed to cool before analysis (Klapa, Aon et al. 2003).

2.2.7 Glucose concentration measurements

The concentration of glucose in the culture was measured using Merckoquant® Glucose-Test. 100-200 µl of culture was applied to the reaction zone of the test strip. The glucose concentration was measured semiquantitavely as glucose was converted into gluconic acid lactone under the presence of glucose oxidase. The hydrogen peroxide formed reacted with an organic redox indicator to form a blue-green dye, and the concentration of the glucose could be determined by visual comparison of the reaction zone on the test strip with the fields of a color scale (Merck KGaA 2006).

2.3 GC-MS SQ instrumentation

The instrument used for sample analysis was an Agilent Technologies 7890A GC system coupled with an Agilent Technologies 5975 inert Mass Selective Detector. The column in the GC system was an Agilent Technologies J&W DB-5ms, product number 122-5532G. This was a 30 m long capillary column with an inner diameter of 250 µm and a membrane thickness of 0.25 µm. The stationary phase coating the column was a phenyl arylene equivalent to a 5 %- phenyl-methylpolysiloxane, shown in Figure 2-1.

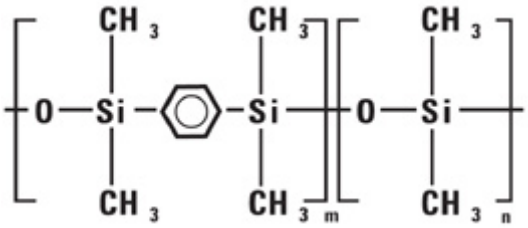

Figure 2-1: The molecular structure of the stationary phase of the column in the GC, Phenyl Arylene polymer virtually equivalent to a (5%-Phenyl)-methylpolysiloxane (Crawford Scientific 2011).

The injection volume was 1.00 µl with a split ratio of 10:1. The injector was set to a constant flow of 0.90029 ml/min, and the injector temperature was set to 250 °C. The transfer line between the GC and the MS was set to 300 °C. The oven was set to 60 °C for 1 minute for equilibration, then heated 10 °C per minute to 325 °C and kept at this temperature for 10 minutes for a total of 37.5 minutes of cycle time. The MS was set to scan mode, ranging from 50.0 to 600.0 m/z. The lower threshold for recording abundances was 150. A delay of 7 minutes was set for the MS to avoid unnecessary detection of solvent. The temperature of the MS source was set to 230 °C and the temperature of the MS quadrupole was set to 150 °C.

3 Results and discussion

The overall goal for this thesis was to establish experimental protocols for analysis of the metabolome and the fluxome of *S.cerevisiae*. The metabolites of the cells are the focus for both types of analysis; one focuses on the presence and concentration of metabolites (metabolome analysis) and the other focuses on the conversion of one metabolite to another (fluxome analysis), and the same experimental platform can often be used for both.

The experimental methodologies can be divided into three parts; growing of cells, sampling and extraction of metabolites, and analysis of the metabolites by GC - MS. The analytical part of the protocols was the same for all experiments, while the cultivation of cells and sampling of metabolites differed. Any refinements to the experimental protocols are commented at the end of each chapter.

3.1 Creation of a Deconvolution Reporting Software (DRS) library

A custom DRS library with a selection of metabolites found in *S. cerevisiae* was created to allow an automated and fast way of quantifying metabolites in a sample. 20 µl of 10 mM stock solution of selected metabolites was derivatized with MTBSTFA and analyzed using GC – MS. The main focus was on amino acids, but some carboxylic acids from the citric acid cycle were analyzed as well. The list of the analyzed compounds is shown in Table 3-1. Aspargine and glutamine were not analyzed, as they are quickly deamidated to aspartate and glutamate, respectively (Antoniewicz, Kelleher et al. 2007).

Table 3-1: Selected metabolites in *S.cerevisiae* for creating the DRS library.

Detected			Not detected
Alanine	Histidine	Phenylalanine	Arginine
Aspartate	Isoleucine	Proline	Fumarate
Citrate	Leucine	Serine	Pyruvate
Cysteine	Lysine	Threonine	Succinate
Glutatmate	Methionine	Tyrosine	α-ketoglutarate
Glycine	Oxaloacetate	Valine	

A typical graphical output of a total-ion chromatogram (TIC) in Chemstation (the software used for handling GC – MS data) is shown in Figure 3-1 for a mixture of stock solutions of valine, threonine and glutamate derivatized with MTBSTFA.

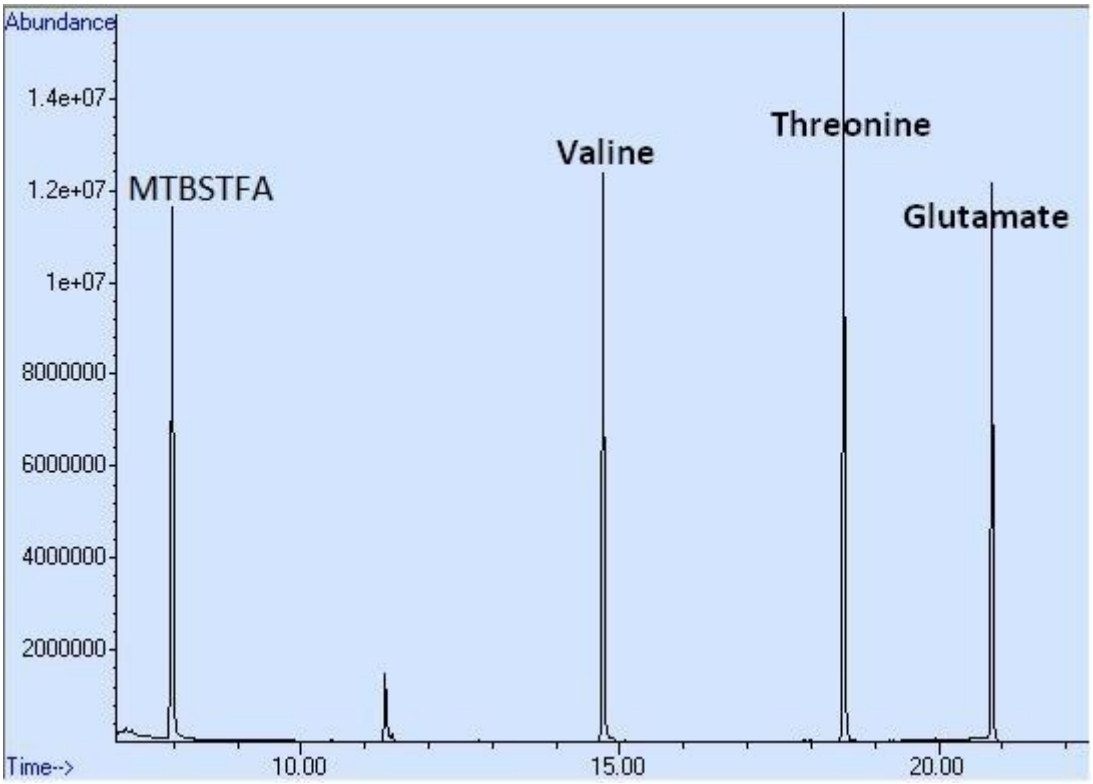

Figure 3-1: Total ion chromatogram in Chemstation for a solution containing valine, threonine and glutamate.

The amino acids were identified by comparing the mass spectra for each peak with previously determined mass spectra in the literature (Antoniewicz, Kelleher et al. 2007), and their retention times were determined. The leftmost peak in the figure is unreacted derivatization agent, while the other peaks were identified as valine (RT=14.378 min), threonine (RT=18.515 min), and glutamate (RT=20.842 min). The fragmentation pattern of valine eluting at 14.738 minutes is shown in Figure 3-2.

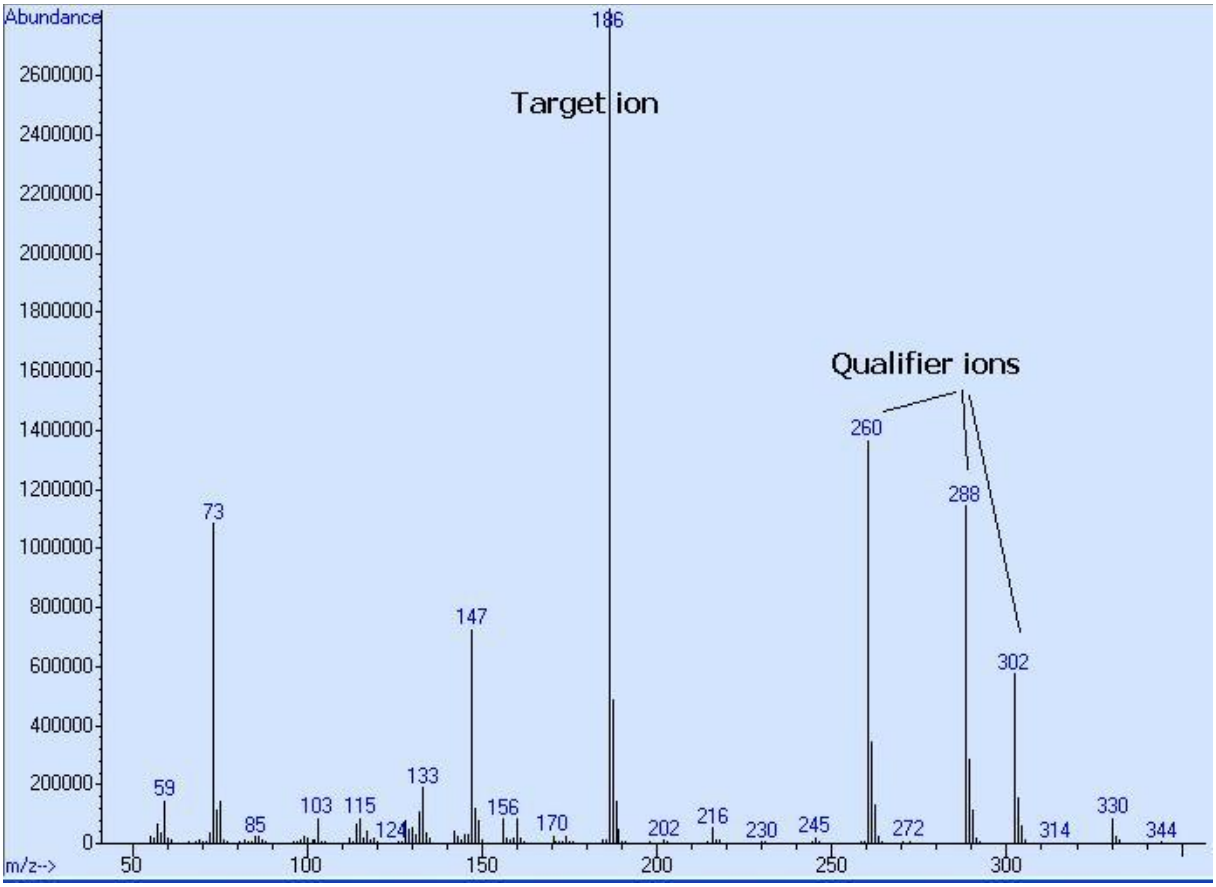

Figure 3-2: The mass spectrum of MTBSTFA-derivatized valine, showing target ion and qualifier ions.

The target ion is manually selected by the operator, generally as the ion with the highest response, which for valine was the ion with m/z of 186. Qualifier ions are used in addition to the target ion to identify the compound, based on their response relative to the target ion. For co-eluting compounds, a unique set of target and qualifier ions is needed for each compound to allow accurate identification.

Out of the 23 selected metabolites, 18 were detected and their retention times and fragmentation patterns (Table 3-2) were added to the DRS library.

Table 3-2: Data for retention times, target ions and qualifier ions of the metabolites used for creation of a DRS library.

Metabolite	Retention time [min]	Target ion [m/z]	Qualifier ion 1 [m/z]	Qualifier ion 2 [m/z]	Qualifier ion 3 [m/z]
Alanine	13.358	158	232	260	147
Glycine	13.708	147	218	246	73
Valine	14.738	186	260	288	302
Leucine	15.186	200	274	302	147
Isoleucine	15.482	200	302	274	147
Proline	16.006	184	258	286	147
Methionine	18.035	218	292	320	244
Serine	18.215	390	288	362	302
Threonine	18.515	303	404	376	417
Phenylalanine	19.225	302	308	336	234
Oxaloacetate	19.663	417	389	459	207
Aspartat	19.778	302	418	316	390
Cysteine	20.246	302	378	406	448
Glutamate	20.842	432	330	272	358
Lysine	21.78	300	198	272	329
Histidine	23.411	196	440	338	73
Citrate	23.57	459	591	431	357
Tyrosine	23.799	302	466	438	364

All the metabolites were distinguishable by the combination of retention time and mass spectra. The only exception was leucine and isoleucine, which due to identical molecular mass and a very similar molecular structure were hard to distinguish from one another. They eluted closely together and the identical molecular mass made the fragmentation patterns identical for both. For simplicity leucine was here defined as the compound to elute first from the GC column with isoleucine eluting approximately 17 seconds later.

Data for the metabolites were added to the library, which was then used to quantify the metabolites in samples taken from cultures of *S. cerevisiae*. This is shown in Figure 3-3 for a

sample taken from a culture stressed with 5FU, with alanine highlighted. In AMDIS, a hit in the database is marked by a "T" above the TIC (Figure 3-3 A), with the other parts of the window showing information about the highlighted metabolite (Figure 3-3 B-E).

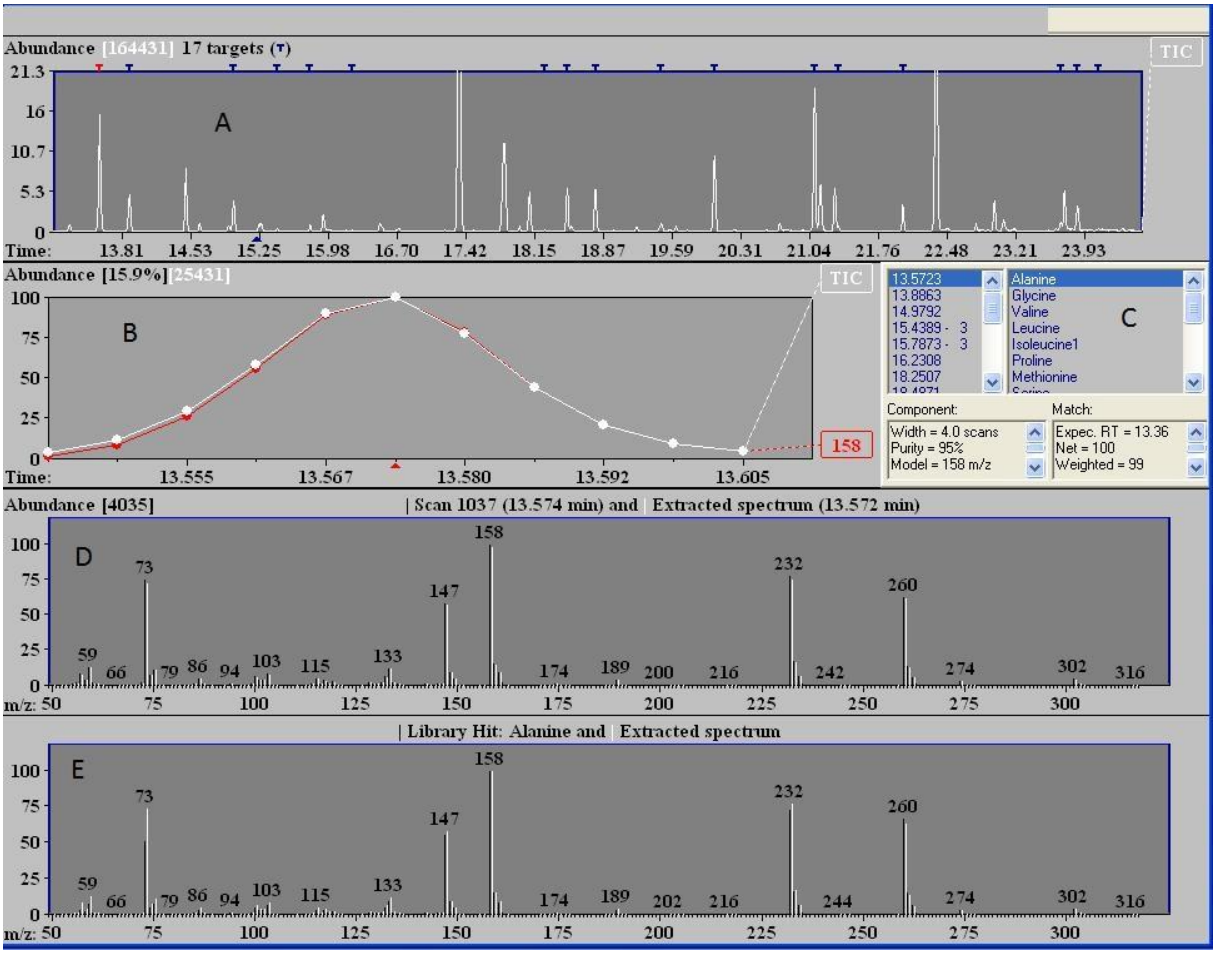

Figure 3-3: Graphical representation of data obtained by GC – MS analysis of MTBSTFA-derivitized metabolites in AMDIS, screened against the DRS library. A: Total-ion chromatogram, a "T" marks a recognized metabolite. B: Component display showing the portion of the chromatogram directly used in the deconvolution. C: Component data list showing information about hits in the DRS library. D: Component mass spectral display (Scan Display), black bars showing the raw MS and white bars showing the deconvoluted MS. E: Target mass spectral display (Library display), black bars showing MS from the library and white bars showing the component spectrum.

After the automatic quantification with the DRS library, the results were manually validated. Especially the ratios of the target/qualifier ions (Figure 3-3 E) were checked and, when needed, parameters involved in quantification were adjusted.

A typical TIC of a sample taken from a culture of *S. cerevisiae*, e.g. Figure 1-13, will contain more peaks than can be identified by the use of this created DRS library. To provide a more detailed view of the metabolome of *S. cerevisiae*, the library could be expanded to include a wider range of metabolites, thus allowing identification of more peaks.

3.2 Determination of cultivation parameters

Biomass samples were to be harvested during the exponential growth phase at an OD_{600} of 8-10 to ensure a high enough concentration of cells for the detection of intracellular metabolites. An estimation of when the culture is the mid-exponential phase is when OD is at about 50 % of the maximal value, and therefore a final OD_{600} of about 15 or above was desirable.

To determine the concentration of glucose needed to reach a final OD_{600} of 15 or above a series of fermentations were performed with glucose concentrations ranging from 5 g/l to 80 g/l. Figure 3-4 shows the growth curves for cells grown at different glucose concentrations, see appendix 6.1 for data.

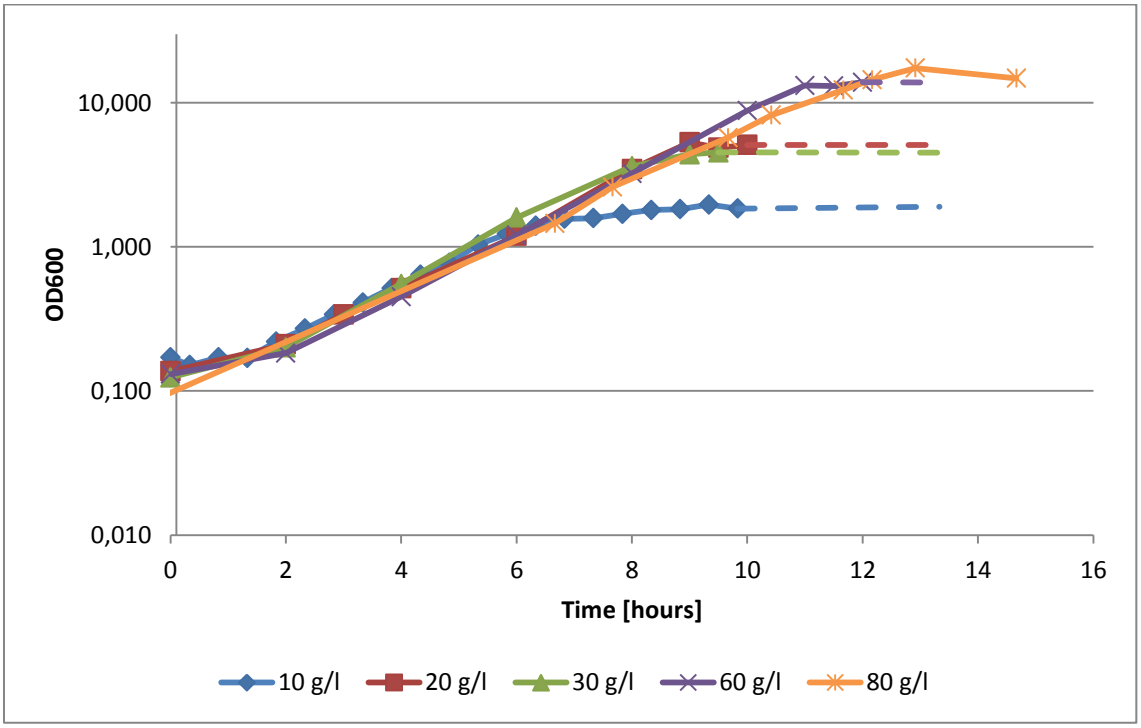

Figure 3-4: The growth curve of *S. cerevisiae* growing in media with different glucose concentrations. Dashed lines are added as an estimate of the maximum concentration for easier comparison.

As expected, a higher glucose concentration generally yielded a higher maximum final concentration of cells in the culture. Since the concentrations of the other ingredients in the media were unchanged, and the biomass yields were similar for all the cultures, the concentration of glucose was presumed to be the limiting factor for maximum OD in this series of cultivations. For all subsequent fermentations a glucose concentration of 80 g/l was used, giving a maximum value of OD_{600} of about 17.

Experiments performed by fellow student A.M. Haug (unpublished) have shown that for this strain the ratio between OD_{600} and dry weight (DW) per liter was about 2.5:1. The maximum growth rate μ_{max} and the biomass yield Y_{XS} (gram biomass produced per gram glucose consumed) was calculated, and is shown in Table 3-3. See appendix 6.2 for examples of calculation.

Table 3-3: Exponential growth rate and biomass yield for aerobic growth of cells in a bioreactor with different glucose concentrations.

	Glucose concentration [g/l]				
	10	**20**	**30**	**60**	**80**
μ_{max} [h^{-1}]	0,43	0,43	0,48	0,48	0,46
Y_{XS} [g biomass/ g glucose]	0,076	0,10	0,060	0,093	0,087

The growth rates were slightly higher than previously reported growth rates for *S. cerevisiae* CEN.pk of 0.41 h^{-1} (grown in shake flasks) (van Dijken, Bauer et al. 2000), while the biomass yields were lower than the reported 0.12 g/g for aerobic batch cultivation in a bioreactor from the same study. The higher growth rate could be a consequence of better conditions for growth in a bioreactor than in shake flasks, as parameters like pH and O_2-saturation are under better control in a bioreactor. Due to the limited amount of experiments performed, the growth rate and yield presented here cannot be considered definite and were only used as guiding numbers.

Experimental protocol refinement

Different sampling protocols were tested during these cultivations. Following the boiling ethanol extraction, a method for freeze-drying was explored. Briefly explained, the samples in ethanol were frozen - 80 °C in a tilted position to maximize the surface area of the ethanol-

sample mixture. The frozen samples were placed in the freeze-dryer, and a vacuum was applied at room temperature for 24 hours. However, the ethanol-sample mixture melted before the freeze-drying completed, probably due to an insufficient surface area-to-volume ratio. To reduce the risk of melting, bigger tubes could be used or the samples could be spread out to more tubes to increase this ratio. However, further attempts at freeze-drying were not made, as the alternative method of using a Speedvac turned out to be a much simpler and more time-efficient method.

3.3 Osmotic stressing of cells

The response of osmotic stress has been widely investigated in yeast, and its response to osmotic stress is one of the best understood signaling networks in eukaryotic cells (de Nadal, Alepuz et al. 2002; Hohmann 2002). At severe salt stress (1 M NaCl) a "typical" upregulated yeast gene involved in osmotic stress response will be maximally induced at 30-60 minutes (Martinez-Montanes, Pascual-Ahuir et al. 2010). Although unable to determine changes in gene expression with the methods described here, an experiment of osmotic stressing would serve as a quick, safe and cheap way of gaining experience in and, if necessary, refine the methods for cultivation in the bioreactor, addition of stress agent, sampling, extraction and analysis of intracellular metabolites.

In aerobic growth of *S. cerevisiae*, glucose is oxidized to carbon dioxide and water in an exergonic reaction, as described by the simplified reaction:

$C_6H_{12}O_6 + O_2 = 6\ CO_2 + H_2O + \text{energy}$

The consumption of O_2 and the production of CO_2 increase as the culture grows to a higher concentration. The levels of O_2 and in particular CO_2 are useful for estimating the growth of the cells in the culture, as the continuous readings (once every second) of the air leaving the fermenter give an immediate indication on the level of respiration in the culture, and hence the growth of the cells.

Osmotic stress was applied to the cells by addition of NaCl to a total concentration of 1 M at OD_{600}=8, approximately nine hours after inoculation. The cultivation progress is illustrated in Figure 3-5, see appendix 6.1 for data.

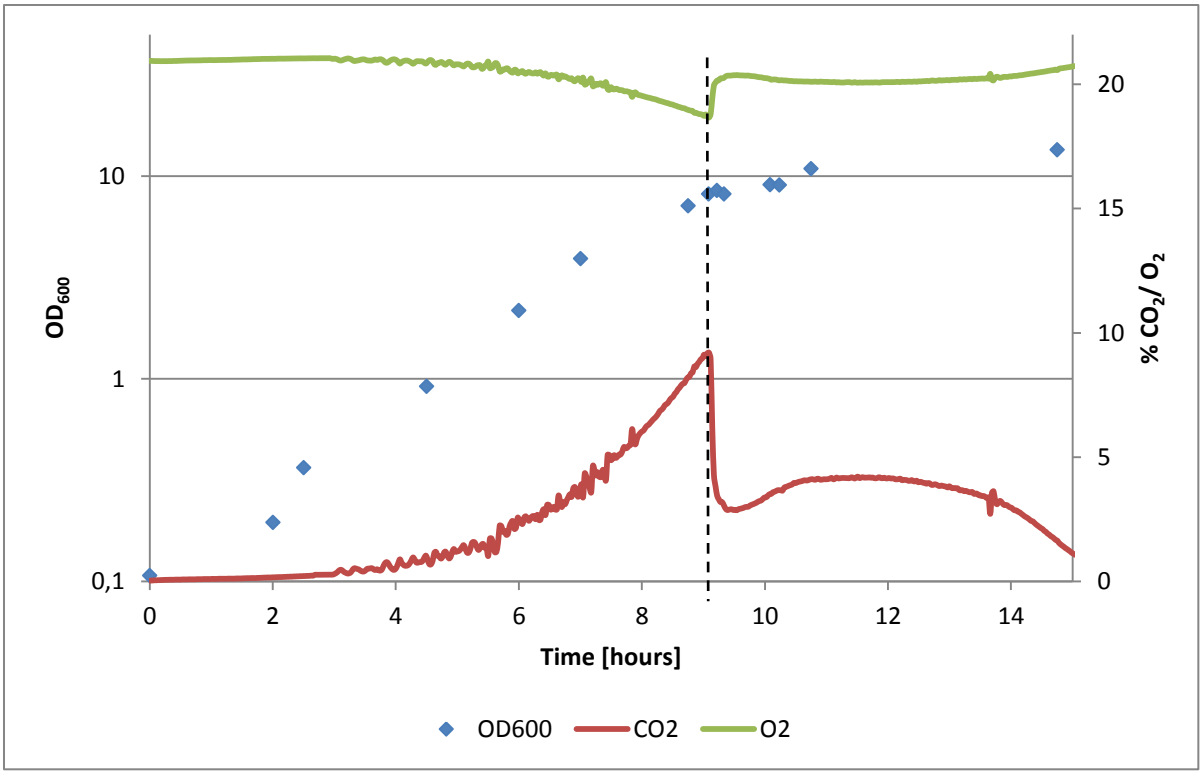

Figure 3-5: The cultivation progress of *S. cerevisiae* osmostressed by addition of 1M NaCl. The dashed vertical line indicates when the salt was added to the culture. The CO_2 and oxygen levels of the air out of the fermenter are also shown.

As the osmotic stress was applied (the dashed vertical line in Figure 3-5), an immediate response was observed. The osmotic stress hindered respiration, causing less CO_2 to be produced, consumption of less oxygen and a halt in exponential growth. The sudden drop in CO_2 was followed by a slow rise, indicating that the cells were slowly adjusting to the new environment and trying to resume growth before eventually succumbing to the harsh environment, characterized by the slow decrease in CO_2 levels occurring from 12 hours and after. The final concentration of cells was lower than for an unstressed culture, OD_{600}=13 versus OD_{600}=17, indicating that the cells ability to grow had been hindered and the energy from the glucose no longer was being utilized for growth, but rather for pathways involved in stress response.

Samples were taken from the culture at 30 seconds, 5 minutes and 60 minutes after addition of salt, and the intracellular metabolites were analyzed (Figure 3-6, see appendix 6.3 for data).

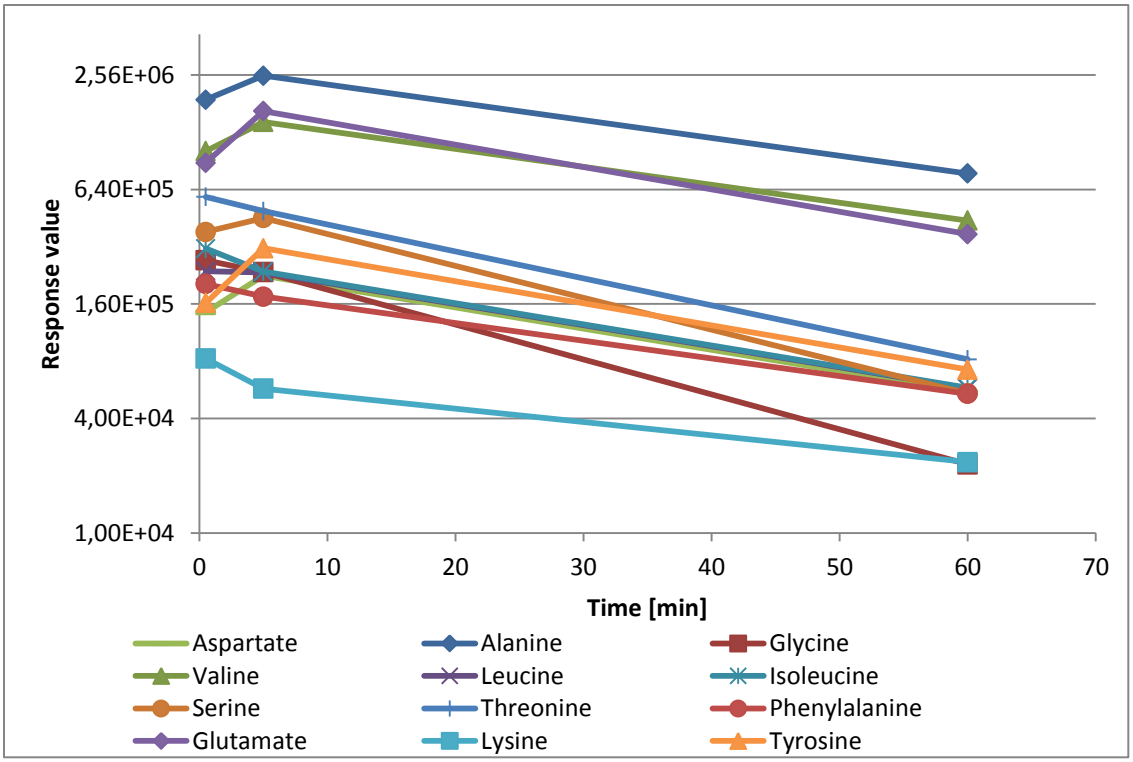

Figure 3-6: Response values from GC – MS analysis of metabolites from a culture of *S. cerevisiae* stressed with 1M NaCl.

Screening the data obtained from analysis with GC – MS against the DRS library showed 12 hits out of the 19 metabolites in the library. Being a semi-quantative method, it was not attempted to determine the exact concentrations of the different metabolites. The response values are a measure of ion concentrations detected by the mass spectrometer in the GC – MS, but equal amounts of two different compounds do not necessarily give the same response value. A more suitable approach was to look at the trends of the response values for the amino acids over time to determine whether the amount of the intracellular metabolites have increased or decreased.

The amino acids could be divided into two groups, according to the immediate response to the osmotic stress. The amount of alanine, glutamate, valine, serine, tyrosine, aspartate and proline increased 5 minutes after addition of stress compared to 0.5 minutes after stress, while the amount of glycine, leucine, threonine, phenylalanine and lysine all decreased. Thus, a change in the composition of the total pool of amino acids occurred after the stress, possibly as a part of the immediate cellular response to the osmotic stress. As the reactions involved in metabolic response to stress are many, it can be challenging to determine the specific role of each amino acid. One hour after the addition of salt, all the amino acids were present in a

lower amount than the previous two sampling points, indicating a decrease in total amino acid pool as a result of the osmotic stress. This is in agreement with previous studies, where amino acid starvation was observed during the lag phase occurring after being subjected to osmotic stress (Pandey, Yoshikawa et al. 2007). This is possibly linked to an increased demand of amino acids due to redistribution of intracellular concentration of different enzymes involved in increasing the osmotic tolerance of the cell (Pandey, Yoshikawa et al. 2007). The availability of amino acids has been shown to be interconnected to the cells tolerance to osmotic stress (Pascual-Ahuir, Serrano et al. 2001), and a continuous decrease in intracellular amino acid pool could explain the lack of steady regrowth in the hours after the time of salt addition. However, such a decrease was not confirmed as the last sample was taken only 1 hour after addition of salt. To further investigate this relation between amino acids and stress tolerance, samples should be taken for several hours after time of stress. Osmotic tolerance was however not a focus for this thesis, and this was not pursued any further.

Experimental protocol refinement

No samples were taken before the addition of salt, and a comparison of the stressed cells versus cells under exponential growth was not possible. This led to a correction in the sampling protocol, and for future experiments samples would also be taken a few minutes before the addition of the stress agent. Additionally, the sample volume was increased from the initial 5 ml to 8 ml as it proved difficult to pipette 2x2 ml from 5 ml of sample without disturbing the precipitated cell walls. By taking samples of 8 ml, 3x2 ml could be pipetted out safely, which also gave the benefit of one extra parallel.

D3- alanine was added as an internal standard to all samples after extraction with boiling ethanol as a means of determining the amount of metabolites lost during processing. However, d3-alanine was not detected by GC – MS, neither for samples derivatized with MTBSTFA nor samples derivatized with MCF (performed by A.M. Haug). A possible explanation was that the d3-alanine was somehow compromised, either because the solution used was contaminated or simply mislabeled, or d3-alanine was broken down during the sample processing before analysis by GC – MS.

The results obtained were satisfactory, in that the analysis of the samples taken showed a range of detected metabolites, and the sampling protocol had been refined.

3.4 Analysis of changes in the metabolome of *S. cerevisiae* as a response to addition of 5FU

Once all the necessary protocols for cultivation, sampling and analysis had been developed, the cellular response of *S. cerevisiae* to 5FU was examined. The cells were inoculated in the bioreactor, and DNA damage was introduced to the cells by addition of 0.5 mM 5FU total concentration when the culture reached OD_{600}=10. The cultivation progress is illustrated in Figure 3-7, see appendix 6.1 for data.

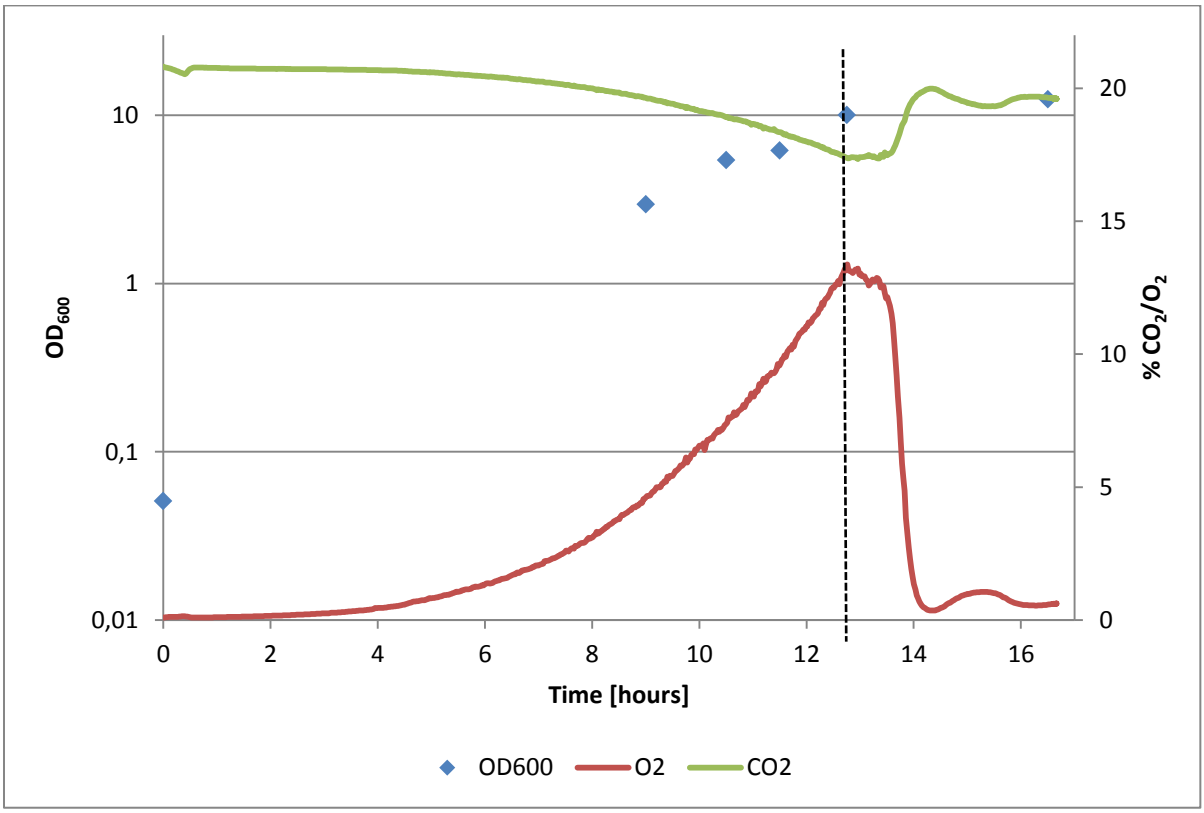

Figure 3-7: The cultivation progress of *S. cerevisiae* stressed by addition of 0.5 mM 5-fluorouracil. The dashed vertical line indicates when the agent was added.

The growth of the cells were clearly affected by the addition of the DNA damaging agent, as the characteristic exponential increase of CO_2 levels of a culture during exponential growth phase was interrupted. For 40 minutes after addition of 5FU, the CO_2 levels slowly decreased as a consequence of the DNA damage caused by 5FU inducing cell cycle arrest, and energy from oxidizing glucose no longer being used for cell growth but rather for pathways involved in protecting against the damage caused. Approximately 40 minutes after the addition of 5FU, the CO_2 levels dropped to almost nothing, probably as a result of depletion of glucose in the medium that would completely stop all respiration of the cells. The final OD_{600} of the culture

was 12.44, a 25 % increase since 5FU was added. A possible explanation for this increase is that although 5FU induced cell cycle arrest and stopped all growth, the cells that were already undergoing cell division at the time would complete the cell division cycle and form new cells, thus increasing OD_{600} of the culture.

Samples were taken for metabolite analysis by GC - MS in intervals starting from 5 minutes prior to the stress and up to 60 minutes after. The response values for the detected metabolites are shown in Figure 3-8, see appendix 6.3 for data. Generally, all metabolites followed the same trends between sampling points with the exception of the sample taken at 11 minutes. At this sampling point three metabolites; aspartate, glutamate and citrate, showed a decrease in response value whereas the other metabolites showed a clear increase. This difference in trends might be linked to a cellular response of the cells to the DNA damaging agent as DNA repair pathways are activated.

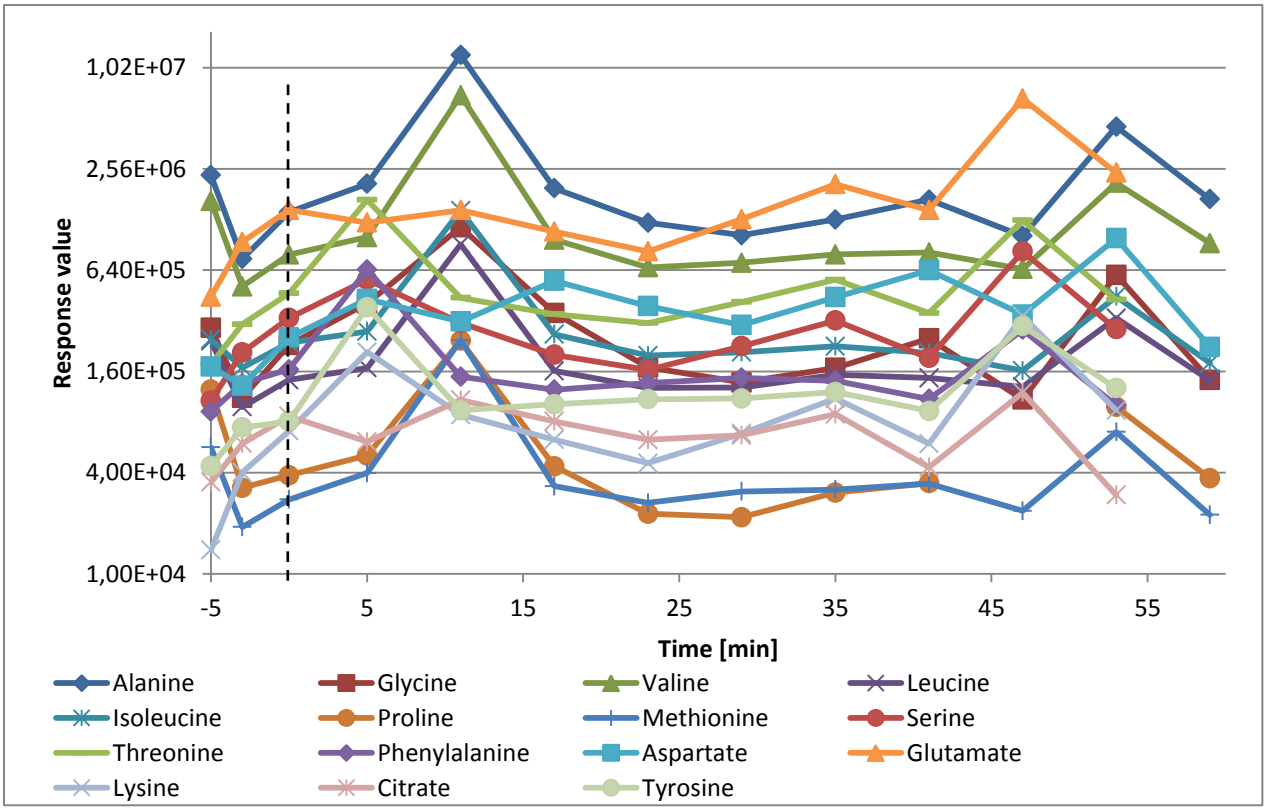

Figure 3-8: Response values for the metabolites detected by GC – MS prior to and after addition of 0.5 mM 5FU to a culture of *S. cerevisiae*. The dashed vertical line indicates the time of 5FU addition.

Similarly, a lower dose of 5FU was added to the culture to examine the metabolic response to a more tolerable amount of 5FU. Figure 3-9 shows the cultivation progress for cells stressed with 0.1 mM 5FU, see appendix 6.1 for data.

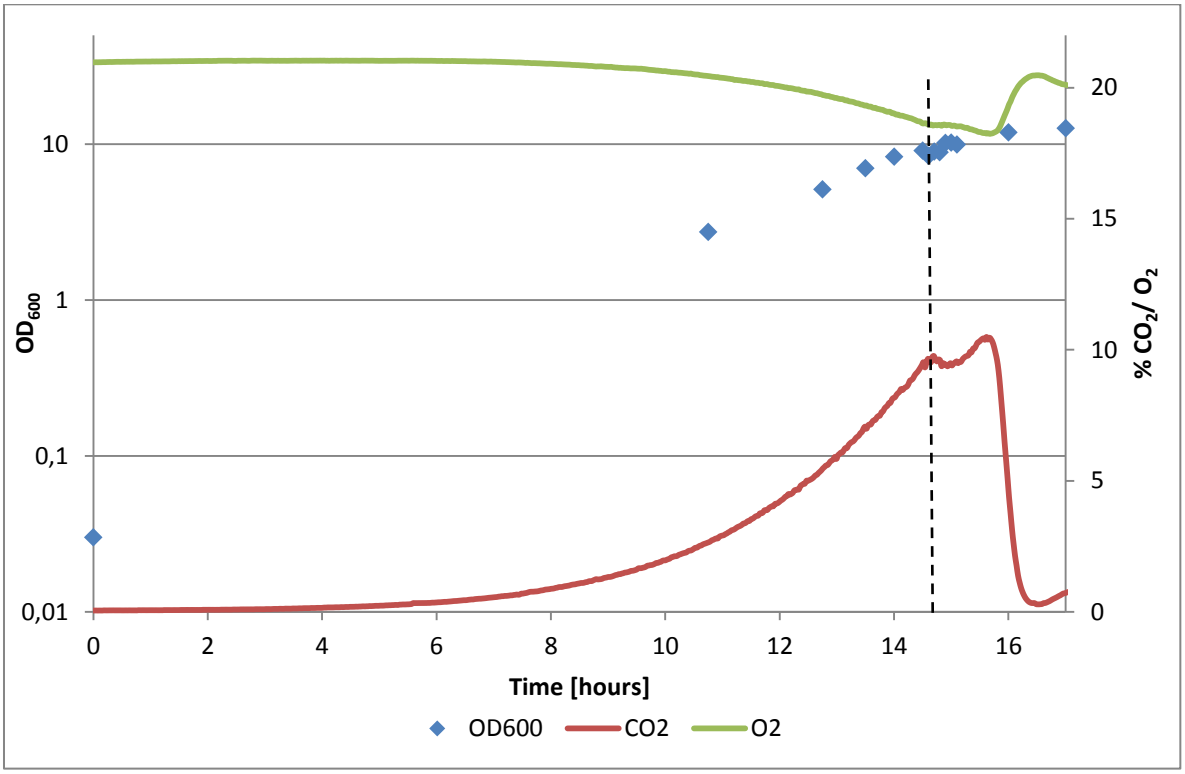

Figure 3-9: Addition 0.1 mM of the DNA damaging agent 5-fluorouracil to a culture of *S. cerevisiae*. The dashed vertical line indicates when the agent was added.

After the addition of 5FU, a slight disturbance of the respiration is observed before the cells continued the exponential growth. After adjusting to the new environment, the cells were able to repair the damage introduced by 5FU and start growth again. The sudden drop in CO_2 that followed approximately 90 minutes later was a consequence of the depletion of glucose in the medium.

Samples were taken for metabolite analysis by GC - MS in intervals starting from 6 minutes prior to the stress and up to 30 minutes after. The response values for the detected metabolites are shown in Figure 3-10, see appendix 6.3 for data.

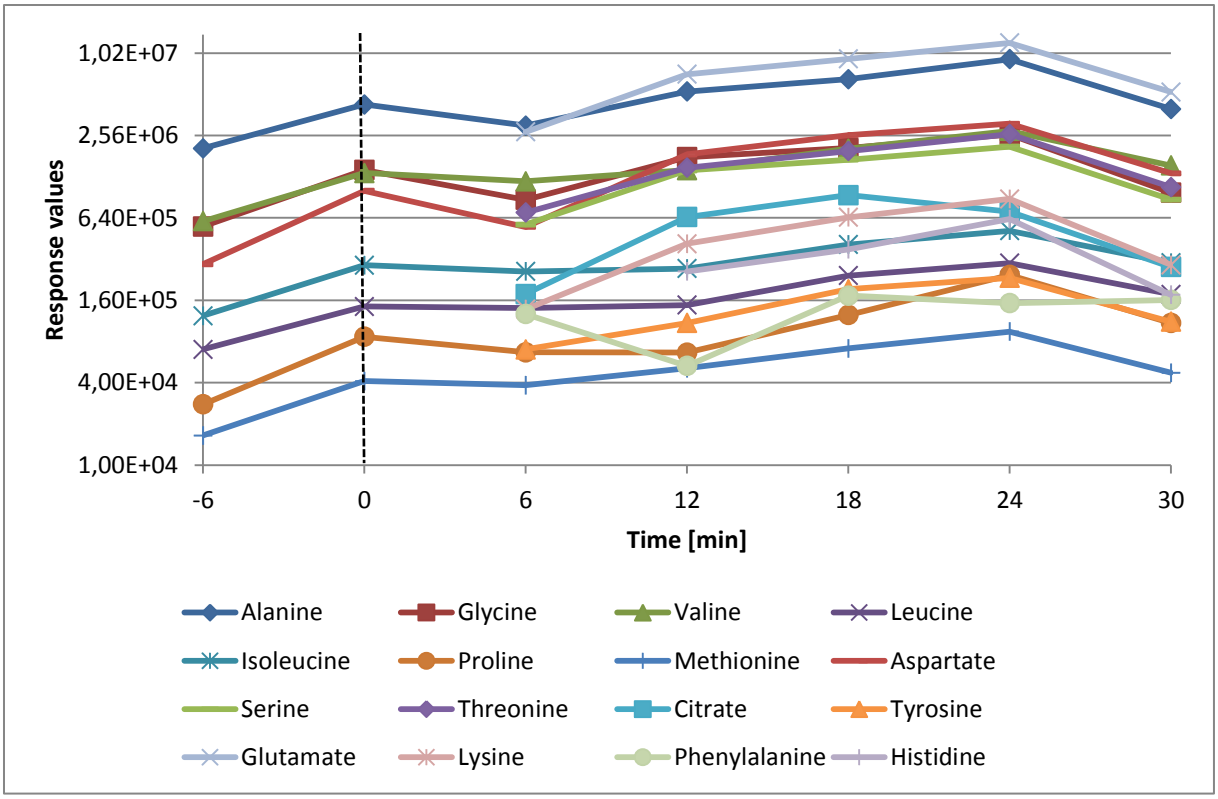

Figure 3-10: Response values for the metabolites detected by GC - MS prior to and after addition of 0.1 mM 5FU to a culture of *S. cerevisiae*. The dashed vertical line indicates the time of 5FU addition.

The effects of 5FU were less prominent as the concentration was lower. Generally, the metabolites showed a slow increase in response value over time, probably as a result of the resumed growth. Contrary to what was observed for growth on 0.5 mM, the three metabolites glutamate, aspartate and citrate show no marked variation in response value compared to the other metabolites. The only metabolite that is showing any sign of deviation from the others is phenylalanine, which showed a decrease in response value 12 minutes after the addition of 5FU, but returned to the same relative level as the others at 18 minutes. This could be a response to the effect of 5FU, but it could also be just a deviation in the data obtained from GC – MS.

3.5 Analysis of metabolic fluxes using FiatFlux

The publicly available software FiatFlux 1.6X allows easy and quick calculation of metabolic fluxes in *S. cerevisiae* based on GC – MS analysis of samples taken from cultures grown on a mixture of 80 % natural glucose and 20 % [U-^{13}C] glucose. The goal of these experiments was to establish a protocol for analysis of the metabolic fluxes, and then use this protocol to determine if a change in the metabolic fluxes of the cells could be observed as a result of growth on medium containing DNA damaging agents.

3.5.1 Experimental conditions for fluxomics

The cultivations for the metabolic flux ratio experiments were performed in 250 ml shake flasks containing 20 ml of medium instead of in a bioreactor. Only one bioreactor was available, while many shake flasks could be used for cultivation at the same time in one incubator. Shake flasks therefore provided a greater flexibility when determining different factors like glucose concentration, anti-cancer drug concentration and growth rate of the cells. The lower volumes also provided an economical benefit, in that smaller amounts of ingredients and stressing agents were needed.

To determine the concentrations needed to stress the cells and still maintain growth, a series of cultivations were performed using different concentrations of either 5FU or MMS. Initially, a concentration of 5 g/l of glucose was used. In an unstressed culture, this would yield an estimated maximum OD_{600}=1.5-1.8. The sampling were to be done at $OD_{600}\leq 1$, so that enough glucose still remained in the medium to avoid a shift in carbon catabolite repression, to which pathways like respiration are subjected to (Zimmermann and Entian 1997). Such a shift can cause up to 15 % decrease in growth rate (Herwig, Doerries et al. 2001), and happens when the source of carbon (glucose in these experiments) is nearing depletion. The results of these cultivations are shown in Figure 3-11, see appendix 6.1 for data.

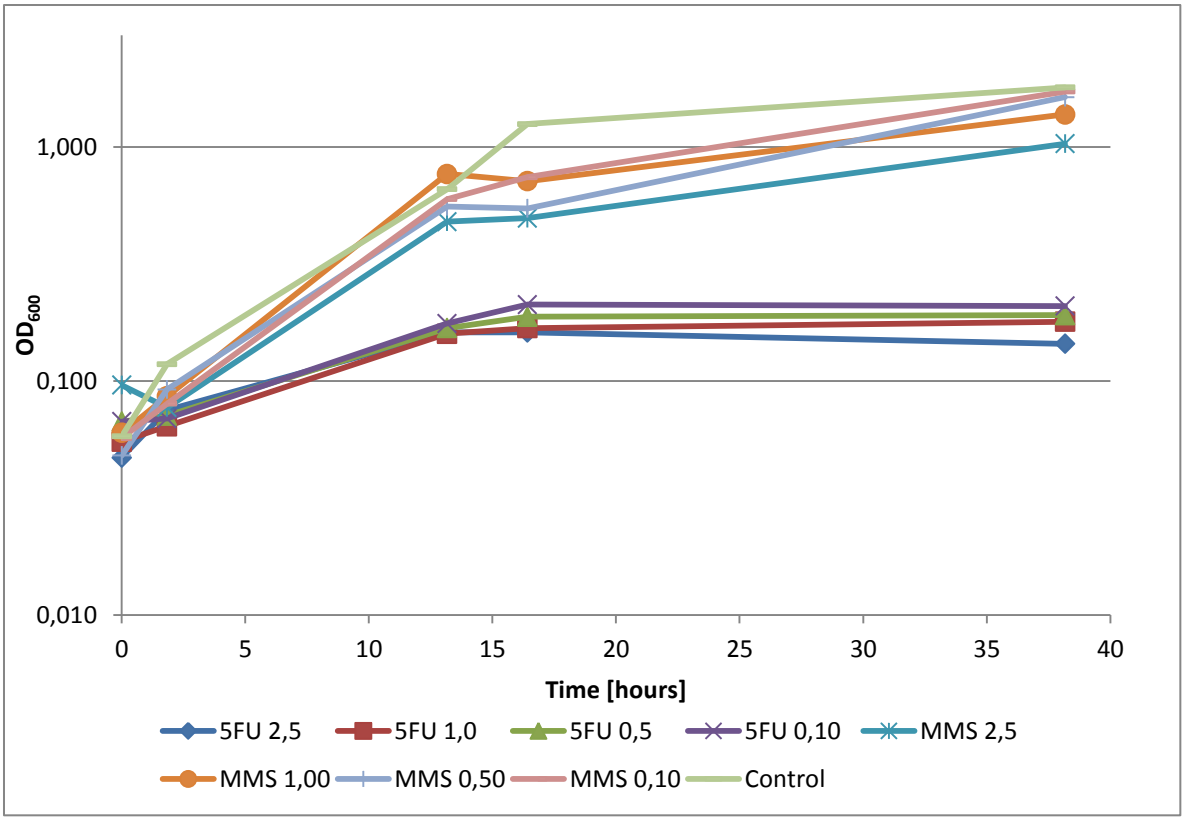

Figure 3-11: OD_{600} measurements for *S. cerevisiae* grown in medium containing 5 g/l glucose and MMS or 5FU. Numbers in the labels indicate the concentration of the DNA damaging agent in mM.

The end concentration of the control culture was OD_{600}=1.8 and exponential growth continued past OD_{600}=1 (time of sampling). For the culture stressed with MMS, an exponential growth phase similar to the control culture was observed for the first 13 hours. Between 13 hours and 16 hours no growth was observed, and glucose test showed that all glucose had been depleted. The cultures were left in the incubator overnight, and 22 hours later the OD_{600} had doubled for all cultures grown on MMS, indicating an additional round of cell division had occurred during the night. A possible explanation for this is linked to accumulation of glycogen and trehalose that occurs in the cells during the late phase of the exponential growth (Lillie and Pringle 1980). Under a non-stress situation, when all carbon sources have been depleted the cell will use the stored trehalose in a protective role (Singer and Lindquist 1998), while the stored glycogen is used for termination of proliferation and replenishment of trehalose (Jorgensen, Olsson et al. 2002). However, for cells treated with MMS it has been suggested that the cells will mobilize the stored carbohydrates to continue growth when all exogenous carbon sources are depleted (Kitanovic, Walther et al. 2009),

which would explain why the cells could resume growth after all glucose in the medium had been consumed.

Since the MMS treated cells had similar growth rates as the control culture for the first 13 hours, raising the glucose concentration was the next logical step to ensure exponential growth beyond the sampling point of OD_{600}=1. An increase of glucose concentration would also lead to an increase in resistance to the damage caused by MMS (Benton, Somasundaram et al. 2006), leading to a growth rate of the stressed cells even closer to that of the unstressed cells. A new series of cultivation with the same amounts of MMS but a glucose concentration of 10 g/L was performed, and the results of this series are shown in Figure 3-12, see appendix 6.1 for data.

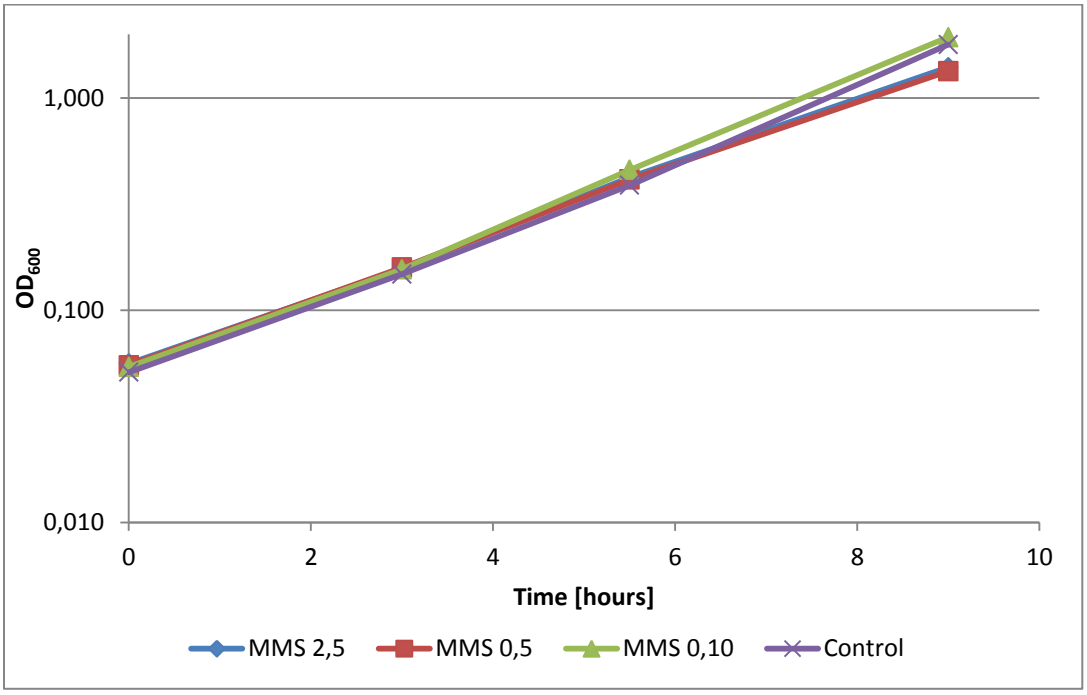

Figure 3-12: OD_{600} measurements for *S. cerevisiae* grown in medium containing 10 g/l glucose and MMS. Numbers in the labels indicate the concentration of the DNA damaging agent in mM.

As can be seen in Figure 3-12, the cells in all the cultures were growing at a very similar rate, and all cultures were in the exponential phase past OD_{600}=1. The highest dose of MMS, 2.5 mM, was chosen for the final experiment with ^{13}C-glucose.

For the cells stressed with 5FU (Figure 3-11), it was evident that the cells did not tolerate the concentrations of the anti-cancer drug, and all growth stopped at $OD_{600} \leq 0.2$. A new series of cultivations with lower concentrations of 5FU was set up. The glucose concentration was raised to 10 g/l to keep the conditions between the experiments done with the two anti-cancer

drugs as consistent as possible. The growth curves of these cultivations are shown in Figure 3-13, see appendix 6.1 for data.

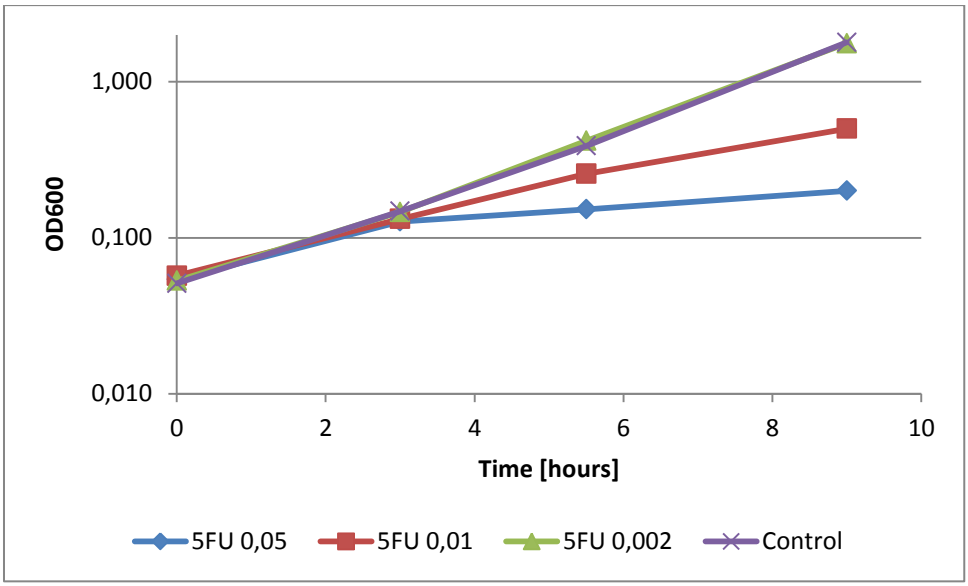

Figure 3-13: OD_{600} measurements for *S. cerevisiae*, grown in medium containing 10 g/l glucose and 5FU. Numbers in the labels indicate the concentration of the DNA damaging agent in mM.

The exponential growth of 0.002 mM was almost identical to the control culture, indicating that the cells were practically unaffected by the added 5FU, while the higher concentrations of 5FU showed a distinctly lower growth rate. For the final experiments, a concentration of 0.005 mM 5FU was chosen as a compromise between the unaffected 0.002 mM culture and the affected 0.01 mM culture.

3.5.2 Determining the change in metabolic flux profile due to growth under stress

To determine the effect the anti-cancer drugs had on the metabolic fluxes in *S. cerevisiae*, cells were cultivated in shake flasks in a medium containing a low concentration of 5FU (0.005 mM) or MMS (2.5 mM). The amount had to be sufficiently high in order to activate stress response pathways, but low enough to allow the cells to overcome the stress and continue exponential growth. In addition to a control culture grown in medium containing 100 % natural glucose, one culture was grown on medium containing 80 % natural glucose and 20 % [U-^{13}C] glucose to determine if the labeled [U-^{13}C] glucose had any effect on the growth rate or biomass yield. The growth curves for the cultures are shown in Figure 3-14, see appendix 6.1 for data.

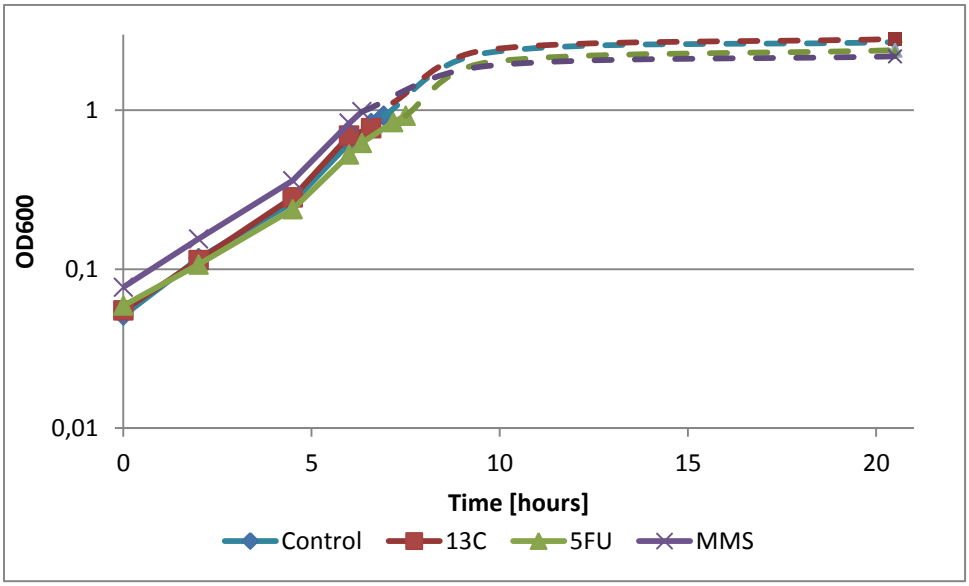

Figure 3-14: OD_{600} measurements for cultures grown on medium containing 10 g/l of 80 % normal glucose and 20 % [U-^{13}C] glucose. The dashed lines are an estimate of the progression of the growth curve after sampling and until the stationary phase is reached.

The growth curves of the cultures were similar in shape, but the cells treated with DNA damaging reagents were growing slightly slower. 20 hours after inoculation all cultures had reached an $OD_{600} \geq 2$, and it was assumed that all the cells were in the exponential phase at the time of sampling ($OD_{600} \approx 1$). An estimated growth curve (dashed lines) was added for each culture beyond the time of sampling to graphically illustrate a typical progression of cell growth in a batch culture, based on the final concentration and the exponential growth rate at the time of sampling. The growth rate during the exponential phase and the biomass yield was calculated for each culture (Table 3-4, see Appendix 6.2 for examples of calculations). The growth rates for the cultures were similar, except for the culture stressed with 5FU growing at

a rate approximately 10 % lower than the control culture. The small differences in growth rates indicated that the cells were able to respond properly to the stress while continuing exponential growth. The biomass yields were lower for the cultures under stress (13 % lower for 5FU and 21 % lower for MMS compared to the control culture), indicating that some energy was being directed away from biomass synthesis and over to stress response pathways. The growth rate and biomass yield of the culture grown on the mix of labeled and natural glucose were almost identical to the control culture, indicating that the labeled glucose had little or no impact on the growth of the cells.

Table 3-4: Exponential growth rate and biomass yield for aerobic growth of cells in shake flasks under various conditions.

	Control	13C	5FU	MMS
μ_{max} [h^{-1}]	0,42	0,44	0,39	0,43
Y_{XS} [g biomass/ g glucose]	0,11	0,11	0,096	0,087

Samples were taken at OD_{600}≈1, analyzed with GC – MS and the metabolic fluxes (Figure 3-15) were calculated using FiatFlux 1.6X.

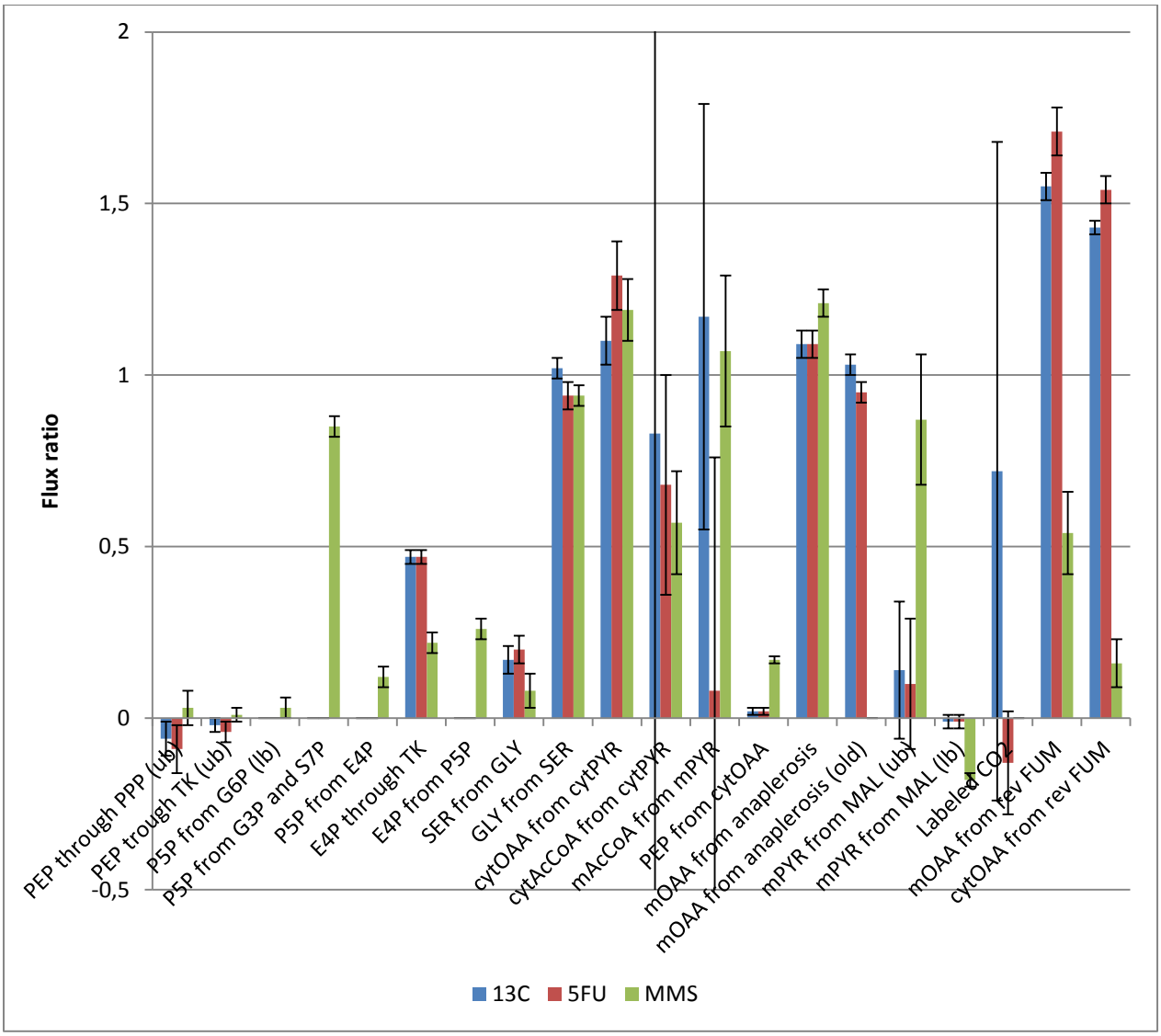

Figure 3-15: Calculated metabolic flux ratios with standard deviations in *S. cerevisiae* during growth under non-stress conditions (13C) or under stressed conditions (5FU or MMS). Abbreviations: PEP, phosphoenol pyruvate; PPP, pentose phosphate pathway; ub, upper bound; TK, transketolase; P5P, pentose 5-phosphates; G6P, glucose 6-phosphate; lb, lower bound; G3P, triose 3-phosphate; S7P, sedoheptulose 7-phosphate; E4P, erythrose 4-phosphate; SER, serine; GLY, glycine; cytOAA, cytosolic oxaloacetate; cytAcCoA, cytosolic acetyl-CoA; cytPYR, cytosolic pyruvate; mAcCoA, mitochondrial acetyl-CoA; mPYR, mitochondrial pyruvate; mOAA, mitochondrial oxaloacetate; MAL, malate; rev FUM, reversible flux from fumarate.

9 out of the 20 available flux ratios in FiatFlux were determined for all three cultivations with small standard deviations, making comparison of these responses to the DNA damaging agents possible.

Many pentose phosphate pathways flux ratios were not determined since most histidine-fragments were not assigned, which was necessary to resolve the MDV_M of the pentoses (Zamboni 2007). The standard deviations for some of the calculated fluxes ("cytAcCoA from cytPYR" and "mAcCoA from mPYR") were so large that they normally should be excluded when interpreting the data. However, they were included here for the sake of providing an example of interpretation of the data, as a wider view of the metabolic activity in the cells allowed a more thorough interpretation of the cellular responses. Obviously, a more complete profile of the metabolic fluxes in the cells is obtained as more fluxes are calculated.

The effect of the anti-cancer drugs on the metabolic fluxes relative to the fluxes of an unstressed culture is graphically illustrated in Figure 3-16 for cells stressed with 5FU and Figure 3-17 for cells stressed with MMS.

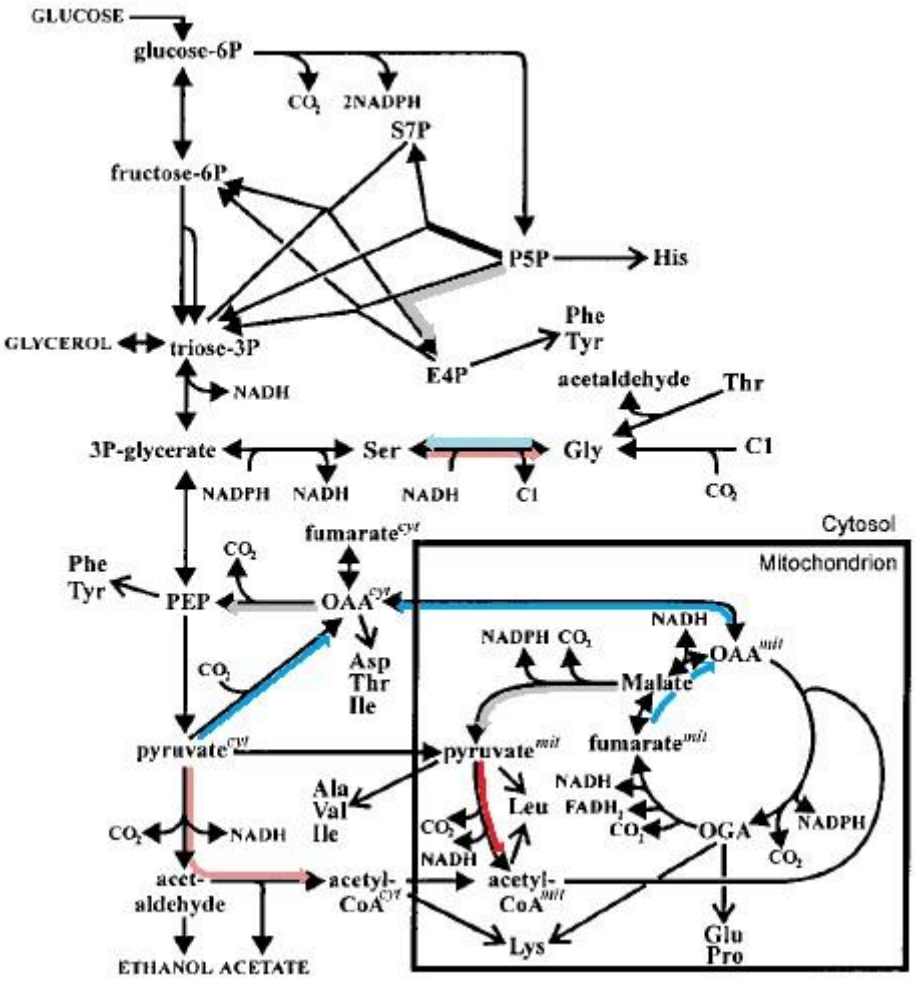

Figure 3-16: The effect of growth in 0.005 mM 5FU on the central carbon metabolism of *S. cerevisiae*. The colored arrows indicate a difference in flux ratio relative to the unstressed cells. Dark blue arrows indicate a marked increase; light blue arrows indicate a slight increase; grey arrows indicate no difference; dark red arrows indicate a marked decrease; light red arrows indicate a slight decrease.

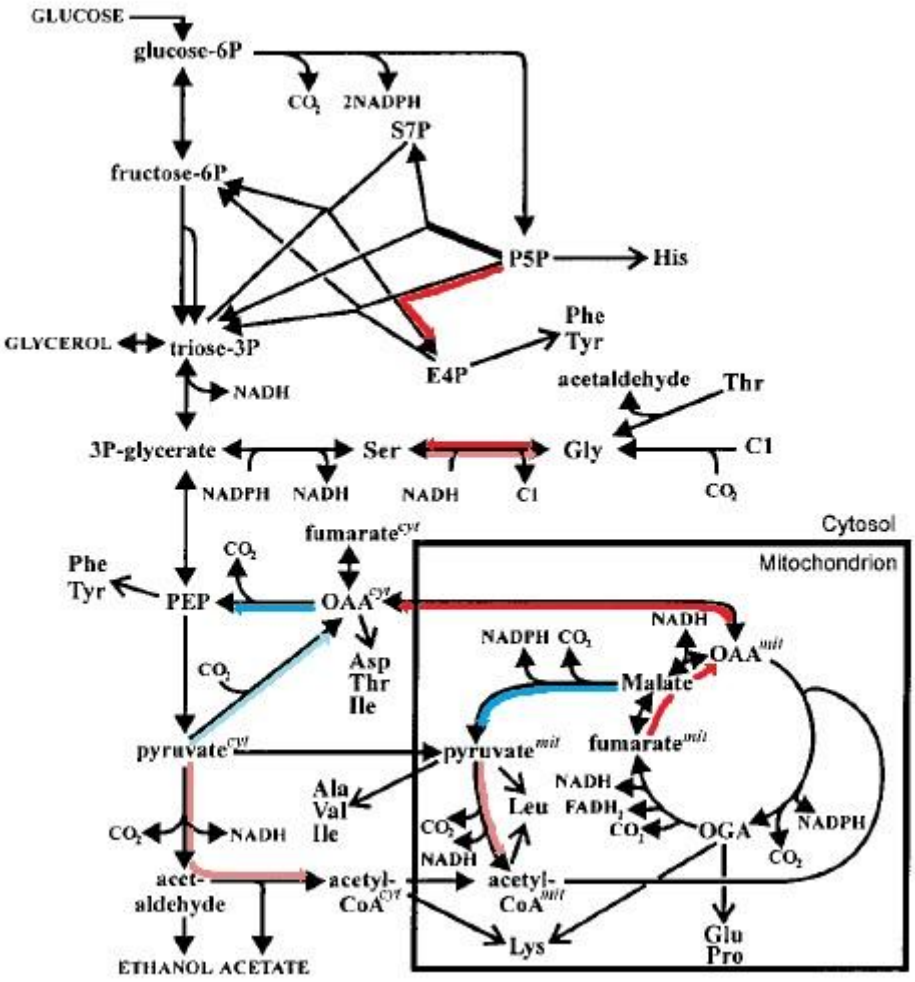

Figure 3-17: The effect of growth in 2.5 mM MMS on the central carbon metabolism of *S. cerevisiae*. The colored arrows indicate a difference in flux ratio relative to the unstressed cells. Dark blue arrows indicate a marked increase; light blue arrows indicate a slight increase; grey arrows indicate no difference; dark red arrows indicate a marked decrease; light red arrows indicate a slight decrease.

Cells from both of the stressed cultures showed a decrease in production of acetyl-CoA, through both the fermentative pathway (producing ethanol, acetate, CO_2 and NADH) and the respiratory pathway (oxidation of mitochondrial pyruvate to acetyl-CoA producing CO_2 and NADH). As acetyl-CoA is the main substrate of the TCA cycle, this reduction could be an indication of a lower activity of the full TCA cycle as a response to the DNA-damage. A lower activity of the TCA cycle could be a result of a lower demand for ATP, as the biomass synthesis is reduced for the stressed cells. For the MMS-stressed cells, a reduction in TCA cycle activity is further backed up by a reduction in the conversion of fumarate to oxaloacetate. However, this is not the case for the 5FU-treated cells, where an increased flux

is observed. This seemingly contradictory observation could be explained by an increased demand of cytosolic oxaloacetate, which is provided by export of mitochondrial oxaloacetate produced from fumarate via malate, with fumarate or malate being replenished by other anaplerotic reactions.

The reason some fluxes were not calculated in FiatFlux was that part of the data obtained from GC – MS had to be excluded due to either MDV_M residuals of dubious quality or the fractional labeling of the metabolites not reflecting that of the substrate. Minimizing these sources of errors is key in providing better results.

The method of derivatization can be optimized to produce better resolution of the amino acid fragments. The method used in this work was adapted from another metabolic flux analysis study (Klapa, Aon et al. 2003), where the mixture of derivatization agent and sample were heated at 60 °C for 30 minutes. The high abundance of unreacted MTBSTFA that was observed in most chromatograms, e.g. Figure 3-1, could indicate that these conditions were not sufficient to allow all MTBSTFA to react with the metabolites. By elevating the temperature and/or extending the reaction time, a more complete derivatization could be achieved, possibly resulting in a higher resolution of the GC – MS data. A higher resolution of GC – MS data will lead to less exclusion of MDV_M fragments in FiatFlux, thus allowing more fluxes to be calculated.

In FiatFlux the user has the option to assign the weight of the amino acid fragments used for calculation of fluxes. A previous study determined which amino acid fragments, when derivatized with MTBSTFA, were acceptable for use for metabolic flux analysis (Antoniewicz, Kelleher et al. 2007) and which fragments should be excluded due to overlapping. Adjusting the amino acid fragment weights in FiatFlux according to their findings could result in more accurate calculation of the fluxes.

Experimental protocol refinement

The proteins were at first hydrolyzed in 6M HCl at 110 °C for 24 hours. This turned out to be problematic as the tubes used for hydrolysis did not withstand the pressure of boiling HCl (boiling point of 6M HCl is 110 °C (Aylward and Findlay 2007)) which resulted in biomass leaking out during the hydrolysis. The temperature needed to be lowered to 100-105 °C to avoid this problem.

3.6 Future prospects

The DRS library can be expanded to include a wider range of metabolites. This will allow a more detailed profile of the metabolome of *S. cerevisiae* when determining the cellular responses to different stress situations, and key metabolites involved in stress response pathways can be identified.

During the cultivation of the cells, measurements of the levels of acetate, ethanol and glucose should be taken to provide extra information of the metabolic activity in the cells. The levels of acetate and ethanol can give an indication on whether the cells prefer aerobic respiration or anaerobic fermentation of glucose to produce energy. The levels of glucose left in the medium can give an indication on the uptake of glucose throughout the cultivation progress. Effects related to glucose, such as the Crabtree effect (aerobic production of alcohol under the presence of high concentrations of glucose) or carbon catabolite repression, can be monitored and, if necessary, adjustments be made to avoid them.

The experiments for metabolic flux analysis can be done in a chemostat to eliminate any effects that specific growth rate might have on the cellular response to the different anti-cancer drugs. When the culture is in a steady state, a pulse of a non-lethal dose of the anti-cancer drugs can be applied to the culture and samples taken in time intervals after the pulse.

4 Conclusions

A custom DRS library was created to allow fast and automated quantification of metabolites in samples from cultures of *S. cerevisiae*. The library contained a selection of 19 metabolites in *S. cerevisiae*, and was used to examine the change in the metabolome of the cells as 5FU was added to a culture during the exponential growth phase. Addition of 0.5 mM 5FU resulted in a decrease of respiration in the culture and a change in the composition of the metabolite pool, as the amount of aspartate, glutamate and citrate decreased compared to the other metabolites between 5 and 11 minutes after time of stress. The cells were able to resume growth after addition of 0.1 mM 5FU after a short period of adjusting to the added stress, and no clear change in the metabolite pool was observed.

Metabolic flux analysis showed that the ratio of the fluxes leading to mitochondrial acetyl-CoA was reduced for cells stressed with either 5FU or MMS, compared to unstressed cells. This could be an indication of a reduced activity of the TCA cycle. A difference in the metabolic flux response was observed for the conversion of fumarate to oxaloacetate in the mitochondria and the subsequent export to the cytosol, where addition of 5FU led to an increase whereas addition of MMS led to a decrease.

5 References

Agilent Technologies Inc. (2007). "Considerations for selecting GC/MS or LC/MS for metabolomics." Retrieved 18.05.2011, from http://www.chem.agilent.com/Library/selectionguide/Public/5989-6328EN.pdf.

Agilent Technologies Inc. (2011). "Deconvolution Reporting Software (DRS) details." Retrieved 19.05.2011, from http://www.chem.agilent.com/en-US/Products/software/chromatography/ms/deconvolutionreporting/Pages/DRSdetails.aspx.

Aherne, G. W., A. Hardcastle, et al. (1996). "Immunoreactive dUMP and TTP pools as an index of thymidylate synthase inhibition; effect of tomudex (ZD1694) and a nonpolyglutamated quinazoline antifolate (CB30900) in L1210 mouse leukaemia cells." Biochemical pharmacology **51**(10): 1293-1301.

Antoniewicz, M. R., J. K. Kelleher, et al. (2007). "Accurate assessment of amino acid mass isotopomer distributions for metabolic flux analysis." Anal Chem **79**(19): 7554-7559.

Aylward, G. H. and T. J. Findlay (2007). SI Chemical Data, John Wiley & Sons Australia, Limited.

Benton, M. G., S. Somasundaram, et al. (2006). "Analyzing the dose-dependence of the Saccharomyces cerevisiae global transcriptional response to methyl methanesulfonate and ionizing radiation." BMC genomics **7**: 305.

Berglund, A. C., E. Sjölund, et al. (2008). "InParanoid 6: eukaryotic ortholog clusters with inparalogs." Nucleic Acids Research **36**(Database issue): D263-D266.

Bornholdt, S. (2005). "Systems biology. Less is more in modeling large genetic networks." Science **310**(5747): 449-451.

Buchholz, A., J. Hurlebaus, et al. (2002). "Metabolomics: quantification of intracellular metabolite dynamics." Biomolecular engineering **19**(1): 5-15.

Campbell Science (2011). "GC Reagents, MTBSTFA." Retrieved 18.03.2011, from http://www.campbellscience.com/MTBSTFA.html.

Canelas, A. B., A. ten Pierick, et al. (2009). "Quantitative evaluation of intracellular metabolite extraction techniques for yeast metabolomics." Analytical chemistry **81**(17): 7379-7389.

Crawford Scientific (2011). "Agilent Technologies J&W DB-5ms." Retrieved 21.03.2011, from http://www.crawfordscientific.com/Agilent_J_W_DB-5ms.htm.

de Nadal, E., P. M. Alepuz, et al. (2002). "Dealing with osmostress through MAP kinase activation." EMBO reports **3**(8): 735-740.

Delaney, J. C. and J. M. Essigmann (2004). "Mutagenesis, genotoxicity, and repair of 1-methyladenine, 3-alkylcytosines, 1-methylguanine, and 3-methylthymine in alkB Escherichia coli." Proceedings of the National Academy of Sciences of the United States of America **101**(39): 14051-14056.

Dinglay, S., S. C. Trewick, et al. (2000). "Defective processing of methylated single-stranded DNA by E. coli AlkB mutants." Genes & development **14**(16): 2097-2105.

Emmerling, M., M. Dauner, et al. (2002). "Metabolic flux responses to pyruvate kinase knockout in Escherichia coli." Journal of bacteriology **184**(1): 152-164.

Feng, X., L. Page, et al. (2010). "Bridging the gap between fluxomics and industrial biotechnology." Journal of biomedicine & biotechnology **2010**: 460717.

Fischer, E. and U. Sauer (2003). "Metabolic flux profiling of Escherichia coli mutants in central carbon metabolism using GC-MS." European journal of biochemistry / FEBS **270**(5): 880-891.

Ghoshal, K. and S. T. Jacob (1994). "Specific inhibition of pre-ribosomal RNA processing in extracts from the lymphosarcoma cells treated with 5-fluorouracil." Cancer research **54**(3): 632-636.

Goffeau, A., B. G. Barrell, et al. (1996). "Life with 6000 genes." Science **274**(5287): 546, 563-547.

Grob, R. L. and E. F. Barry, Eds. (2008). Modern practice of gas chromatography. New Jersey, John Wiley & Sons, Inc.

Herwig, C., C. Doerries, et al. (2001). "Quantitative analysis of the regulation scheme of invertase expression in Saccharomyces cerevisiae." Biotechnology and bioengineering **76**(3): 247-258.

Hitzeman, R. A., F. E. Hagie, et al. (1981). "Expression of a human gene for interferon in yeast." Nature **293**(5835): 717-722.

Hohmann, S. (2002). "Osmotic stress signaling and osmoadaptation in yeasts." Microbiology and molecular biology reviews : MMBR **66**(2): 300-372.

Jorgensen, H., L. Olsson, et al. (2002). "Fed-batch cultivation of baker's yeast followed by nitrogen or carbon starvation: effects on fermentative capacity and content of trehalose and glycogen." Applied microbiology and biotechnology **59**(2-3): 310-317.

Karhumaa, K., R. Garcia Sanchez, et al. (2007). "Comparison of the xylose reductase-xylitol dehydrogenase and the xylose isomerase pathways for xylose fermentation by recombinant Saccharomyces cerevisiae." Microbial cell factories **6**: 5.

Kelley, M. R., Y. W. Kow, et al. (2003). "Disparity between DNA base excision repair in yeast and mammals: translational implications." Cancer research **63**(3): 549-554.

Kiefer, P., E. Heinzle, et al. (2004). "Comparative metabolic flux analysis of lysine-producing Corynebacterium glutamicum cultured on glucose or fructose." Applied and environmental microbiology **70**(1): 229-239.

Kitanovic, A., T. Walther, et al. (2009). "Metabolic response to MMS-mediated DNA damage in Saccharomyces cerevisiae is dependent on the glucose concentration in the medium." FEMS yeast research **9**(4): 535-551.

Klapa, M. I., J. C. Aon, et al. (2003). "Ion-trap mass spectrometry used in combination with gas chromatography for high-resolution metabolic flux determination." BioTechniques **34**(4): 832-836, 838, 840 passim.

Kouzminova, E. A. and A. Kuzminov (2006). "Fragmentation of replicating chromosomes triggered by uracil in DNA." Journal of molecular biology **355**(1): 20-33.

Lab Dom AVMM (Suisse) Inc. (2011). "Study of yeast." Retrieved 24.03.2011, from http://www.vegetal-placenta.com/index2.php?Content=Study.

Lillie, S. H. and J. R. Pringle (1980). "Reserve carbohydrate metabolism in Saccharomyces cerevisiae: responses to nutrient limitation." Journal of bacteriology **143**(3): 1384-1394.

Longley, D. B., D. P. Harkin, et al. (2003). "5-fluorouracil: mechanisms of action and clinical strategies." Nature reviews. Cancer **3**(5): 330-338.

Lopez-Camarillo, C., M. Lopez-Casamichana, et al. (2009). "DNA repair mechanisms in eukaryotes: Special focus in Entamoeba histolytica and related protozoan parasites." Infection, genetics and evolution : journal of molecular epidemiology and evolutionary genetics in infectious diseases **9**(6): 1051-1056.

Martinez-Montanes, F., A. Pascual-Ahuir, et al. (2010). "Toward a genomic view of the gene expression program regulated by osmostress in yeast." Omics : a journal of integrative biology **14**(6): 619-627.

McMaster, M. C. (2008). GC/MS - A practical user's guide. Hoboken, New Jersey, John Wiley & Sons, Inc.

Melese, T. and P. Hieter (2002). "From genetics and genomics to drug discovery: yeast rises to the challenge." Trends in pharmacological sciences **23**(12): 544-547.

Merck KGaA (2006). Glucose test informational pamphlet. M. KGaA. Darmstadt, Germany.

Nanchen, A., T. Fuhrer, et al. (2007). "Determination of metabolic flux ratios from 13C-experiments and gas chromatography-mass spectrometry data: protocol and principles." Methods in molecular biology **358**: 177-197.

Pandey, G., K. Yoshikawa, et al. (2007). "Extracting the hidden features in saline osmotic tolerance in Saccharomyces cerevisiae from DNA microarray data using the self-organizing map: biosynthesis of amino acids." Applied microbiology and biotechnology **75**(2): 415-426.

Pascual-Ahuir, A., R. Serrano, et al. (2001). "The Sko1p repressor and Gcn4p activator antagonistically modulate stress-regulated transcription in Saccharomyces cerevisiae." Molecular and cellular biology **21**(1): 16-25.

Patton, J. R. (1993). "Ribonucleoprotein particle assembly and modification of U2 small nuclear RNA containing 5-fluorouridine." Biochemistry **32**(34): 8939-8944.

Regis Technologies Inc. (2008). "GC derivatization reagents." Retrieved 18.03.2011, from http://www.registech.com/Library/Catalog/GC_Derivatization_2008.pdf.

Santi, D. V. and L. W. Hardy (1987). "Catalytic mechanism and inhibition of tRNA (uracil-5-)methyltransferase: evidence for covalent catalysis." Biochemistry **26**(26): 8599-8606.

Sauer, U., D. R. Lasko, et al. (1999). "Metabolic flux ratio analysis of genetic and environmental modulations of Escherichia coli central carbon metabolism." Journal of bacteriology **181**(21): 6679-6688.

Singer, M. A. and S. Lindquist (1998). "Multiple effects of trehalose on protein folding in vitro and in vivo." Molecular cell **1**(5): 639-648.

Solomon, D. J. S. and S. M. Fischer (2010). "Metabolomics at Agilent: Driving value with comprehensive solutions." Retrieved 18.05.2011, from http://www.agilent.com/labs/features/Agilent_metabolomics.pdf.

Swiss Federal Insitute of Technology Zürich (2008). "Dynamics of Cellular Regulation." Retrieved 16.06.2011.

Szczebara, F. M., C. Chandelier, et al. (2003). "Total biosynthesis of hydrocortisone from a simple carbon source in yeast." Nature biotechnology **21**(2): 143-149.

Szyperski, T. (1995). "Biosynthetically directed fractional 13C-labeling of proteinogenic amino acids. An efficient analytical tool to investigate intermediary metabolism." European journal of biochemistry / FEBS **232**(2): 433-448.

Taylor, E. M. and A. R. Lehmann (1998). "Conservation of eukaryotic DNA repair mechanisms." International journal of radiation biology **74**(3): 277-286.

van Dijken, J. P., J. Bauer, et al. (2000). "An interlaboratory comparison of physiological and genetic properties of four Saccharomyces cerevisiae strains." Enzyme and microbial technology **26**(9-10): 706-714.

van Winden, W. A., C. Wittmann, et al. (2002). "Correcting mass isotopomer distributions for naturally occurring isotopes." Biotechnology and bioengineering **80**(4): 477-479.

Verduyn, C., E. Postma, et al. (1992). "Effect of benzoic acid on metabolic fluxes in yeasts: a continuous-culture study on the regulation of respiration and alcoholic fermentation." Yeast **8**(7): 501-517.

Wahl, A., M. El Massaoudi, et al. (2004). "Serial 13C-based flux analysis of an L-phenylalanine-producing E. coli strain using the sensor reactor." Biotechnology progress **20**(3): 706-714.

Wiechert, W., O. Schweissgut, et al. (2007). "Fluxomics: mass spectrometry versus quantitative imaging." Current opinion in plant biology **10**(3): 323-330.

Wohlhueter, R. M., R. S. McIvor, et al. (1980). "Facilitated transport of uracil and 5-fluorouracil, and permeation of orotic acid into cultured mammalian cells." Journal of cellular physiology **104**(3): 309-319.

Worley, J. and S. Kvech (1999). "More Information on the ICP-MS." Retrieved 22.03.2011, from http://www.seaes.manchester.ac.uk/research/facilities/agu/equipment/ICP_MS/moreinfo/.

Wyatt, M. D. and D. L. Pittman (2006). "Methylating agents and DNA repair responses: Methylated bases and sources of strand breaks." Chemical research in toxicology **19**(12): 1580-1594.

Yoshioka, A., S. Tanaka, et al. (1987). "Deoxyribonucleoside triphosphate imbalance. 5-Fluorodeoxyuridine-induced DNA double strand breaks in mouse FM3A cells and the mechanism of cell death." The Journal of biological chemistry **262**(17): 8235-8241.

Zamboni, N. (2007). FiatFlux 1.6X - Getting started. Zürich, Institute of Molecular Systems Biology.

Zamboni, N., E. Fischer, et al. (2005). "FiatFlux--a software for metabolic flux analysis from 13C-glucose experiments." BMC bioinformatics **6**: 209.

Zimmermann, F. K. and K.-D. Entian, Eds. (1997). Yeast Sugar Metabolism: Biochemistry, Genetics, Biotechnology, and Applications. Lancaster, Techonomic Publishing Company, Inc.

6 Appendices

6.1 Data for growth curves of cells grown in a bioreactor or in shake flasks

Measurements of OD_{600} were done throughout the cultivations in the bioreactor, and are shown in Table 6-1. The inoculation concentration for the cells grown at 80 g/l was lower than for the other cultivations, and the time has been adjusted so that all cultures are at OD_{600}=0.100-0.200 at time=0 hours for easier comparison of the growth curves.

Table 6-1: OD measurements for *S. cerevisiae* grown in a bioreactor on different concentrations of glucose

Glucose concentration [g/l]					
10		**20**		**30**	
Time [hours]	**OD(600)**	**Time [hours]**	**OD(600)**	**Time [hours]**	**OD(600)**
0,0	0,171	0,0	0,137	0,0	0,124
0,3	0,151	2,0	0,211	2,0	0,201
0,8	0,171	3,0	0,340	4,0	0,553
1,3	0,169	4,0	0,517	6,0	1,60
1,8	0,220	6,0	1,19	8,0	3,63
2,3	0,271	8,0	3,47	9,0	4,39
2,8	0,339	9,0	5,32	9,5	4,52
3,3	0,411	9,5	4,87		
3,8	0,517	10,0	5,11		
4,3	0,639				
4,8	0,773	**60**		**80**	
5,3	1,04	**Time [hours]**	**OD(600)**	**Time [hours]**	**OD(600)**
5,8	1,23	0,0	0,131	-2,0	0,043
6,3	1,40	2,0	0,183	6,7	1,45
6,8	1,56	4,0	0,450	7,7	2,61
7,3	1,58	6,0	1,21	9,7	5,73
7,8	1,70	8,0	3,23	10,4	8,22
8,3	1,80	10,0	8,82	11,7	12,3
8,8	1,82	11,0	13,2	12,2	14,4
9,3	1,97	11,5	13,1	12,9	17,4
9,8	1,84	12,0	13,9	14,7	14,8

To determine the appropriate concentration of anti-cancer drugs, cultivations were done in shake flasks and the OD_{600} measurements are for these experiments are shown in Table 6-2.

Table 6-2: OD measurements for *S. cerevisiae* grown in shake flasks for determining appropriate amount of anti-cancer drugs.

Concentration [mM]									
	5FU				MMS				Control
Time [hours]	**2,50**	**1,00**	**0,50**	**0,10**	**2,50**	**1,00**	**0,50**	**0,10**	**-**
0	0,047	0,055	0,067	0,067	0,096	0,060	0,048	0,057	0,058
2	0,075	0,064	0,071	0,069	0,077	0,086	0,092	0,080	0,118
13	0,161	0,159	0,168	0,176	0,479	0,766	0,556	0,598	0,659
16	0,161	0,168	0,188	0,212	0,496	0,713	0,546	0,742	1,25
38	0,144	0,179	0,191	0,209	1,03	1,38	1,63	1,72	1,80

When the appropriate concentrations of the anti-cancer drugs had been determined, a new series of cultivations were performed and the OD_{600} measurements are shown in Table 6-3.

Table 6-3: OD measurements of *S. cerevisiae* grown in shake flasks for metabolic flux analysis.

Time [hours]	**Control**	**13C**	**5FU 0,005 mM**	**MMS 2,5 mM**
0,0	0,051	0,055	0,059	0,077
2,0	0,117	0,114	0,107	0,155
4,5	0,262	0,283	0,238	0,361
6,0	0,622	0,692	0,526	0,83
6,3	-	-	0,624	0,98
6,6	0,83	0,77	-	-
6,9	0,922	-	-	-
7,2	-	1,118	0,84	-
7,5	-	-	0,924	-
20,5	2,6875	2,81	2,39	2,185

6.2 Calculation of biomass yield and growth rates

Growth and biomass yields were calculated for the cultivations of *S. cerevisiae*, and example of such a calculation is shown in equations 6.1 and 6.2.

$$\mu_{max} = \frac{\ln(x_2) - \ln(x_1)}{\Delta t} \rightarrow \mu_{max}(80\text{g glc/l}) = \frac{\ln(8.22) - \ln(1.45)}{(10.4 - 6.6)\text{ h}} = 0.46\ \text{h}^{-1} \quad (6.1)$$

$$Y_{XS} = \frac{\frac{OD_{600}}{OD_{600}/\text{g DW l}^{-1}}}{\text{g glucose l}^{-1}} \rightarrow Y_{XS}(80\text{g glucose l}^{-1}) = \frac{\frac{17.44}{2.5/\text{g DW l}^{-1}}}{80\text{ g glucose l}^{-1}}$$

$$= 0.087\ \text{g DW}/\text{g glucose} \quad (6.2)$$

6.3 Data from analysis with GC – MS

All samples were derivatized with MTBSTFA and analyzed with GC – MS. The data are shown in Table 6-4, Table 6-5 and Table 6-6. The sampling points are relative to the time of addition of stress agent.

Table 6-4: Response values of MTBSTFA-dervatized metabolites from analysis with GC – MS, taken from a culture of *S. cerevisiae* stressed with NaCl.

Response values [1]							
Time [min]	**Alanine**	**Glycine**	**Valine**	**Leucine**	**Isoleucine**	**Proline**	**Methionine**
0,5	1,90E+06	2,71E+05	1,02E+06	2,38E+05	3,13E+05	3,41E+04	3,54E+04
5	2,54E+06	2,36E+05	1,45E+06	2,34E+05	2,37E+05	4,25E+04	-
60	7,76E+05	2,30E+04	4,39E+05	5,75E+04	5,80E+04	-	-
Time [min]	**Serine**	**Threonine**	**Phenylalanine**	**Aspartate**	**Glutamate**	**Lysine**	**Tyrosine**
0,5	3,83E+05	5,85E+05	2,04E+05	1,45E+05	8,84E+05	8,27E+04	1,62E+05
5	4,53E+05	4,93E+05	1,75E+05	2,26E+05	1,65E+06	5,74E+04	3,14E+05
60	5,42E+04	8,19E+04	5,40E+04	5,51E+04	3,73E+05	2,36E+04	7,24E+04

[1] Metabolites that were not detected in some samples are indicated with a minus sign (-)

Table 6-5: Response values of MTBSTFA-derivatized metabolites from analysis with GC - MS, taken from a culture of *S. cerevisiae* stressed with 0.5 mM 5FU.

	Response value							
Time [min]	**Alanine**	**Glycine**	**Valine**	**Leucine**	**Isoleucine**	**Proline**	**Methionine**	**Aspartate**
-5	2,35E+06	2,91E+05	1,65E+06	2,42E+05	2,48E+05	1,25E+05	5,66E+04	1,71E+05
-3	7,47E+05	1,11E+05	5,12E+05	9,84E+04	1,69E+05	3,25E+04	1,90E+04	1,32E+05
0	1,42E+06	2,30E+05	7,93E+05	1,42E+05	2,37E+05	3,86E+04	2,77E+04	2,54E+05
5	2,09E+06	4,06E+05	1,01E+06	1,68E+05	2,77E+05	5,06E+04	3,97E+04	4,31E+05
11	1,22E+07	1,15E+06	7,02E+06	9,12E+05	1,45E+06	2,44E+05	2,45E+05	3,17E+05
17	1,97E+06	3,56E+05	9,73E+05	1,61E+05	2,66E+05	4,36E+04	3,32E+04	5,53E+05
23	1,23E+06	1,69E+05	6,65E+05	1,28E+05	1,99E+05	2,28E+04	2,65E+04	3,91E+05
29	1,03E+06	1,38E+05	7,08E+05	1,28E+05	2,08E+05	2,17E+04	3,09E+04	3,02E+05
35	1,28E+06	1,68E+05	7,95E+05	1,53E+05	2,26E+05	3,04E+04	3,17E+04	4,42E+05
41	1,68E+06	2,51E+05	8,16E+05	1,46E+05	2,06E+05	3,46E+04	3,44E+04	6,39E+05
47	1,02E+06	1,09E+05	6,50E+05	1,30E+05	1,62E+05	-	2,37E+04	3,48E+05
53	4,57E+06	6,00E+05	2,12E+06	3,32E+05	4,46E+05	9,85E+04	6,99E+04	9,91E+05
59	1,69E+06	1,42E+05	9,26E+05	1,41E+05	1,79E+05	3,70E+04	2,25E+04	2,24E+05
Time [min]	**Serine**	**Threonine**	**Citrate**	**Tyrosine**	**Glutamate**	**Lysine**	**Phenylalanine**	
-5	2,06E+05	4,05E+05	4,61E+04	1,41E+05	6,22E+05	3,69E+04	2,33E+05	
-3	1,07E+05	1,76E+05	3,51E+04	4,37E+04	4,45E+05	1,39E+04	9,21E+04	
0	2,07E+05	3,06E+05	5,96E+04	7,43E+04	9,43E+05	4,01E+04	1,36E+05	
5	3,33E+05	4,66E+05	8,65E+04	8,07E+04	1,46E+06	7,07E+04	1,64E+05	
11	5,61E+05	1,68E+06	6,11E+04	3,85E+05	1,23E+06	2,08E+05	6,46E+05	
17	3,11E+05	4,38E+05	1,08E+05	9,39E+04	1,46E+06	8,82E+04	1,49E+05	
23	2,01E+05	3,51E+05	8,07E+04	1,02E+05	1,09E+06	6,29E+04	1,24E+05	
29	1,63E+05	3,10E+05	6,28E+04	1,09E+05	8,28E+05	4,55E+04	1,36E+05	
35	2,26E+05	4,15E+05	6,67E+04	1,10E+05	1,29E+06	6,83E+04	1,46E+05	
41	3,21E+05	5,61E+05	8,91E+04	1,21E+05	2,08E+06	1,10E+05	1,41E+05	
47	1,92E+05	3,56E+05	4,31E+04	9,31E+04	1,46E+06	5,95E+04	1,10E+05	
53	8,28E+05	1,27E+06	1,20E+05	2,98E+05	6,70E+06	3,41E+05	2,82E+05	
59	2,86E+05	4,27E+05	2,95E+04	1,27E+05	2,43E+06	9,39E+04	1,01E+05	

Table 6-6: Response values of MTBSTFA-derivatized metabolites from analysis with GC - MS, taken from a culture of *S. cerevisiae* stressed with 0.1 mM 5FU.

	Response values							
Time [min]	**Alanine**	**Glycine**	**Valine**	**Leucine**	**Isoleucine**	**Proline**	**Methionine**	**Aspartate**
-6	2,06E+06	5,54E+05	6,06E+05	7,00E+04	1,23E+05	2,78E+04	1,65E+04	2,93E+05
0	4,31E+06	1,43E+06	1,36E+06	1,44E+05	2,89E+05	8,66E+04	4,10E+04	1,01E+06
6	3,02E+06	8,67E+05	1,18E+06	1,40E+05	2,60E+05	6,67E+04	3,83E+04	5,50E+05
12	5,35E+06	1,78E+06	1,43E+06	1,47E+05	2,73E+05	6,63E+04	5,10E+04	1,86E+06
18	6,60E+06	2,07E+06	2,05E+06	2,43E+05	4,09E+05	1,25E+05	7,11E+04	2,58E+06
24	9,25E+06	2,60E+06	2,76E+06	2,99E+05	5,15E+05	2,45E+05	9,43E+04	3,12E+06
30	4,00E+06	9,78E+05	1,55E+06	1,77E+05	3,01E+05	1,09E+05	4,72E+04	1,35E+06
Time [min]	**Serine**	**Threonine**	**Citrate**	**Tyrosine**	**Glutamate**	**Lysine**	**Phenylalanine**	**Histidine**
-6	3,50E+05	4,93E+05	1,24E+05	3,81E+04	1,62E+06	6,39E+04	1,03E+05	-
0	9,85E+05	1,08E+06	3,28E+05	9,98E+04	5,50E+06	2,44E+05	1,28E+05	1,04E+05
6	5,73E+05	7,01E+05	1,78E+05	7,00E+04	2,72E+06	1,38E+05	1,27E+05	7,56E+04
12	1,42E+06	1,49E+06	6,49E+05	1,09E+05	7,18E+06	4,14E+05	5,30E+04	2,60E+05
18	1,70E+06	1,97E+06	9,39E+05	1,93E+05	9,28E+06	6,46E+05	1,73E+05	3,77E+05
24	2,12E+06	2,62E+06	7,10E+05	2,33E+05	1,22E+07	8,80E+05	1,52E+05	6,28E+05
30	8,70E+05	1,07E+06	2,80E+05	1,12E+05	5,32E+06	2,90E+05	1,61E+05	1,76E+05

6.4 Abbreviations

Abbreviation	Full name	Unit
μ	Growth rate	h^{-1}
5FU	5-fluorouracil	
cytAcCoA	Cytosylic acetyl coenzyme A	
cytOAA	Cytosylic oxaloacetate	
cytPYR	Cytosylic pyruvate	
dc	Direct current	amp
DRS	Deconvolution Reporting Software	
dTMP	Deoxythymidine monophosphate	
dTTP	Deoxythymidine triphosphate	
dUMP	Deoxyuridine monophosphate	
DW	Dry weight	g
E4P	Erythrose 4-phosphate	
EIC	Extracted-ion chromatogram	
FdUDP	Fluorodeoxyuridine triphosphate	
FdUMP	Fluorodeoxyuridine diphosphate	
FdUTP	Fluorodeoxyuridine monophosphate	
FUDP	Fluorouridine diphosphate	
FUDR	Fluorodeoxyuridine	
FUMP	Fluorouridine monophosphate	
FUTP	Fluorouridine triphophate	
G3P	Triose 3-phosphate	
G6P	Glucose 6-phosphate	
GC	Gas chromatography	
GLY	Glycine	
lb	Lower bound	
LC	Liquid chromatography	
mAcCoA	Mitochondrial acetyl coenzyme A	
mae	Malic enzyme	
MAL	Malate	
MDVA	Mass distribution vector, analyte	
MDVM	Mass distribution vector, metabolite	
MMS	Methyl methanesulfonate	
mOAA	Mitochondrial oxaloacetate	
mPYR	Mitochondrial pyruvate	
MS	Mass spectrometry	
MTBSTFA	*N*-(*tert*-butyldimethylsilyl)-*N*methyl-trifluoroacetamide	
NMR	Nuclear magnetic resonance	
OD	Optical density	
P5P	Pentose 5-phosphates	
PEP	Phosphoenol pyruvate	
PPP	Pentose phosphate pathway	

pyk	Pyruvate kinase	
rev FUM	Reversible flux from fumarate	
RF	Radio frequency	hz
RT	Retention time	minutes
S7P	Sedoheptulose 7-phosphate	
SER	Serine	
t-BDMS	*tert*-butyldimethylsilyl	
TCA	Tri carboxylic acid	
TIC	Total-ion chromatogram	
TK	Transketolase	
TS	Thymidylate synthase	
ub	Upper bound	
vvm	Volume per volume per minute	
Y_{XS}	Biomass yield	gram biomass per gram glucose